SYNTHESIS AND CHARACTERIZATION OF TITANIUM DIOXIDE (TiO_2) DOPED NICKEL OXIDE (NiO) DIELECTRIC MATERIALS

by

NURUL AINON BINTI BAKAR

A report submitted in fulfillment of the requirements for the degree of Bachelor of Applied Science (Materials Technology)

FACULTY OF EARTH SCIENCE
UNIVERSITI MALAYSIA KELANTAN

2017

DECLARATION

I declare that this thesis entitled "**Synthesis and Characterization of Titanium Dioxide (TiO_2) Doped Nickel Oxide (NiO) Dielectric Materials**" is the result of my own research except as cited in the references. The thesis has not been accepted for any degree and is not concurrently submitted in candidature of any other degree.

Signature : _____

Name : Nurul Ainon Binti Bakar

Date : 12th January 2017

ACKNOWLEDGEMENT

First and the foremost, I would like to thank Faculty of Earth Science (FSB), University of Malaysia Kelantan (UMK) in providing me the opportunity to complete this Final Year Project (FYP) in an appropriate and good environment. I would like to thank School of Materials and Mineral Resources Engineering (SMMRE), Universiti Sains Malaysia (USM) for the collaboration with UMK and give the permission to FYP students to use some of their accommodations and machines to complete our experimental works.

Next, I would like to express my deepest gratitude to my helpful and patient supervisor and co- supervisor, Assoc. Prof. Dr. Julie Juliewatty Binti Mohamed and Dr. Muhammad Azwadi Bin Sulaiman for the support, guidance, teaching, encouragements and spend their time throughout these two semesters to complete my final year research project. Then, I am also would like to thank my senior, Muhammad Qusyairie Bin Saari and my fellow friends for valuable sharing and help throughout this research project. Their expertise, valuable comments and constructive suggestions have provided high quality basis for the thesis writing and experimental work.

Last but not least, I would like to show my appreciation to my parents, Mr. Bakar Bin Dollah and Mrs. Rohani Binti Md. Yatim that always supporting me in doing my research project. Finally, thanks to all academic and non-academic who help me during the research either directly or indirectly and also to the laboratory assistants and technicians for guiding me to complete this final year research project.

Synthesis and Characterization of Titanium Dioxide (TiO_2) Doped Nickel Oxide (NiO) Dielectric Materials

ABSTRACT

NiO-based ceramic showed the dielectric constant with the range of $10^3 – 10^5$, but it has high dielectric loss. In this research, TiO_2 act as dopant on NiO and the effect of TiO_2 addition into NiO was investigated. $Ni_{1-x}Ti_xO_{1+x}$ was prepared via solid-state reaction method with different TiO_2 compositions, which are 0.01, 0.02, 0.03, 0.05 and 0.10 mole %. The results of these compositions were compared to the pure NiO composition. The preparation started with the powder mixing process for 24 hours and followed by calcination process at 950 °C for 4 hours. Then, the calcined powders were compacted into 6 mm pellet shape with 250 MPa pressure. Those pellets were sintered at 1250 °C for 5 hours. XRD results showed that sample 1 to 3, which are pure NiO, 0.01 and 0.02 mole % of TiO_2 compositions produced single NiO crystalline phase, while sample 4 to 6, which are 0.03, 0.05 and 0.10 mol % of TiO_2 showed there are secondary TiO_2 phases. Others, SEM analysis showed that increasing TiO_2 concentration make the grain size increase, but 0.02 mole % of TiO_2 gave the largest grain size among all samples, that showed 0.02 mole % is the optimum TiO_2 concentration for grain size enlargement. Furthermore, the increasing of TiO_2 concentration causes decrement trend for bulk density of $Ni_{1-x}Ti_xO_{1+x}$ pellet. In dielectric test, the addition of 0.03 mole % of TiO_2 shows the result of the highest dielectric constant with value of 4.51^{14} and 0.05 mole % of TiO_2 gives the result of lowest dielectric loss with value of 0.53.

Sintensis Dan Pencirian Bahan Dielektrik Titanium Dioksida (TiO_2) Didopkan Dalam Nikel Oksida (NiO)

ABSTRAK

Seramik berasaskan NiO menunjukkan pemalar dielektrik julat 10^3 - 10^5, tetapi ia mempunyai kadar kehilangan dielektrik yang tinggi. Dalam kajian ini, TiO_2 digunakan sebagai pendopan pada NiO dan kesan penambahan TiO_2 ke dalam NiO telah dikaji. $Ni_{1-x}Ti_xO_{1+x}$ telah disediakan melalui kaedah tindak balas keadaan pepejal dengan komposisi TiO_2 yang berbeza, iaitu 0.01, 0.02, 0.03, 0.05 dan 0.10 mol %. Keputusan komposisi ini telah dibandingkan dengan komposisi NiO tulen. Penyediaan dimulakan dengan proses pencampuran serbuk untuk 24 jam dan diikuti dengan proses pengkalsinan pada suhu 950 °C selama 4 jam. Kemudian, serbuk yang dikalsin telah dipadatkan dalam bentuk pelet bersaiz 6 mm dengan tekanan 250 MPa. Pelet-pelet tersebut telah disinter pada suhu 1250 °C selama 5 jam. Keputusan XRD menunjukkan bahawa sampel 1 - 3, iaitu komposisi NiO tulen, 0.01 dan 0.02 mol % TiO_2 menghasilkan fasa kristal tunggal NiO, manakala sampel 4 - 6, iaitu komposisi 0.03, 0.05 dan 0.10 mol % TiO_2 menunjukkan terdapat fasa kedua TiO_2 di dalamnya. Selain itu, analisis SEM menunjukkan bahawa peningkatan kepekatan TiO_2 meningkatkan saiz butiran, tetapi penambahan kepekatan 0.02 mol % memberikan saiz butiran yang terbesar dalam kalangan semua sampel, jadi ia menunjukkan 0.02 mol % merupakan kepekatan TiO_2 yang optimum untuk pembesaran saiz butiran. Kemudian, peningkatan kepekatan TiO_2 juga menyebabkan susutan untuk ketumpatan pukal pelet $Ni_{1-x}Ti_xO_{1+x}$. Dalam ujian dielektrik, penambahan TiO_2 sebanyak 0.03 mol % menunjukkan keputusan pemalar dielektrik paling tinggi dengan nilai 4.51^{14} dan TiO_2 dengan nilai sebanyak 0.05 mol % memberikan keputusan kadar kehilangan dielektrik dengan nilai 0.53.

TABLE OF CONTENTS

LIST OF TABLES

LIST OF FIGURES

LIST OF ABBREVIATIONS

XRD	X-Ray Diffraction
FESEM	Field Emission Scanning Electron Microscopy

LIST OF SYMBOLS

C	Capacitance (F)
t	Thickness of pellet (m)
A	Area of cross section (m^2)
ε	Permittivity
ε_o	Permittivity of vacuum
tan δ	Tangent loss or dissipation factor
D	Dry weight (g)
W	Saturated weight (g)
S	Suspended weight (g)
ρ	Bulk density
°C	Degree Celcius
°C/min	Degree Celcius per minute
Ω	Ohm
K	Kelvin
Hz	Hertz
kHz	Kilo Hertz
MHz	Mega Hertz
GHz	Giga Hertz
Mpa	Mega Pascal
T_c	Curie point
Tc	Critical temperature

CHAPTER 1

INTRODUCTION

1.1 Background of Study

The dielectric materials, which known as insulating materials can be in the form of solid, liquid or gases. Solid dielectrics are the most commonly used in electrical engineering because these materials are very good insulators. Some examples of solid dielectrics are mica, glass, rubber and ceramics. There are good examples of ceramic in dielectric materials, which is Calcium Copper Titanium Oxide (CCTO), Aluminium Oxide (Al_2O_3), Aluminium Nitride (AlN), Silicon Carbide (SiC), Fused Silica (SiO_2) and NiO.

NiO is one of the dielectric materials. NiO is a very important material extensively used in catalysis, battery cathodes, gas sensors, electrochromic films, and magnetic materials (Motlagh et al., 2011). In these applications, it is still needed for synthesizing high quality and ultra-fine powders with required characteristics in terms of their size, morphology, optical properties, magnetic properties and so on (Marselin & Jaya, 2015). NiO is good in insulation, but it needs to be enhance its properties especially in dielectric. In this study, the solid-state or ceramic method is used to synthesis and characterize the TiO_2 doped NiO. By having various amount of TiO_2 added to the NiO, the improvement in phase composition, microstructure, density and dielectric properties will be seen.

1.2 Problem Statement

One of the most commonly used transition metal oxides for a wide range of applications is NiO (Marselin & Jaya, 2015). NiO is an advanced ceramic that can be used in electrical engineering such as capacitors because this material are potentially good insulators. Due to its enormous potential applications such as, anti-ferromagnetic material chemical sensors electrochromic devices, catalysts dye sensitized solar cells (DSSCs), it attracts the researcher's attention towards it (Mallick & Mishra, 2012; Albertst & Lee, 1961; Stamataki et al., 2008; Kamal et al., 2005; Azelee et al., 2009; Bandara & Weerasinghe, 2005).

Ceramics as dielectrics for capacitors have the disadvantage that they are not easily prepared as self-supporting thin plates and, if this achieved, are extremely fragile (Moulson & Herbert, 2003). NiO needs to be improve its dielectric properties because it has high dielectric loss. Thus, the aim of this study is to decrease the dielectric loss, improve the dielectric constant and density of NiO.

1.3 Objectives

1. To synthesis the undoped and TiO_2 doped NiO.
2. To study the effect of different TiO_2 amount on NiO (0.01, 0.02, 0.03, 0.05 and 0.10 mol %).
3. To characterize the samples in term of its phase formation, microstructure, density and dielectric properties.

1.4 Expected Outcomes

The expected result that can be achieved through this study are the synthesis and characterization of undoped and TiO_2 doped NiO with varies TiO_2 composition (0.01, 0.02, 0.03, 0.05 and 0.10 mol %). Doping method opens an effective way to alter the dielectric performance for NiO. The effect of different TiO_2 amount on NiO properties will give us better understanding about doping TiO_2 into NiO system. The undoped and doped NiO samples will be compared their dielectric loss, dielectric constant, density, phase formation and microstructure of NiO.

1.5 Scope of Study

NiO compound has recently attracted the researchers interest due to its high dielectric constant. However, it has high dielectric loss. In order to improve NiO dielectric properties, current study have been focused on the process, properties, structure relationship of the high dielectric properties of NiO by doping with different mole % of TiO_2. Doping method opens an effective way and chance to alter the dielectric performance of NiO. Five different mole % of dopants were selected with variation of doping concentration, which are 0.01, 0.02, 0.03, 0.05 and 0.10 mole % of TiO_2 used. The aim of this experimental work is to investigate the effect of different dopant concentration on the properties of NiO with various TiO_2 compositions. Thus, further study of NiO with different mole % of TiO_2 will be investigated in this project work.

CHAPTER 2

LITERATURE REVIEW

2.1 Introduction

A ceramic is an inorganic, non-metallic solid that made up of either metal or non-metal compounds that have been shaped and then hardened by heating to the high temperature. Generally, their physical properties are hard, corrosion-resistant and brittle. But, nowadays the term 'ceramic' has a more expansive meaning and includes materials like glass, advanced ceramics and some cement systems as well.

Ceramics can be defined as solid compounds that are formed by the application of heat, and sometimes heat and pressure, comprising at least two elements provided one of them is a non-metal or a nonmetallic elemental solid. The other element(s) may be a metal(s) or another nonmetallic elemental solid(s) (Barsoum, 2002).

In addition, ceramic can be divided into two main classes which are traditional and advanced ceramics. Traditional ceramics also known as pottery which is one of the oldest human technology using the clay-based materials. Pottery is based on clay and other siliceous minerals that can be conveniently fired in the 900–1200°C temperature range (Moulson & Herbert, 2003). Others, the major types of pottery can be described as earthenware, stoneware and porcelain.

For the advanced ceramics, they are not generally clay-based. Instead, they are either based on oxides or non-oxides or combination of both oxides and non-oxide. Advanced ceramics excel in terms of their high temperature stability (up to 2500 °C and beyond), high hardness, high corrosion resistance, low thermal expansion and a variety of electrical properties ranging from insulators to semiconductors to high conductive materials (Heimann, 2010).

2.2 Advanced Ceramics

Advanced ceramics differ from conventional ceramics in their high-mechanical strength, fracture toughness, wear resistance, refractory, dielectric, magnetic and optical properties. Advanced ceramics or fine ceramics are high value-added inorganic materials produced from high purity synthetic powders to control microstructure and properties (Patil, 1993).

The first use of ceramics in the electrical industry took advantage of their stability when exposed to extremes of weather and to their high electrical resistivity, a feature of many siliceous materials. The methods developed over several millennia for domestic pottery were refined for the production of the insulating bodies needed to carry and isolate electrical conductors in applications ranging from power lines to the cores bearing wire-wound resistors and electrical fire element (Moulson & Herbert, 2003).

Advanced ceramics are categorized as the electroceramics, glass ceramics, bioceramics and others. The unique properties of electroceramics make it important nowadays especially in the development of electronic, communication, automobile, bio-medicine, energy conversion and storage and others (Hsiao et al., 2007).

2.3 Electroceramics

Electroceramics is one type of advanced ceramics. The electroceramics describe the ceramic materials that have been specially formulated for specific electrical, magnetic or optical properties. The properties can be tailored to operation as insulators, ferroelectric materials, highly conductive ceramics, electrodes as well as sensors and actuators. Common applications for electroceramics are as the insulator, resistor, piezoelectric sonar transducers, ferroelectric thin-film memories, electro-optic light valves, high dielectric constant capacitors, and many more.

Seven types of electroceramic materials are including dielectric, insulators, piezoelectric, ferroelectric, magnetic, superconductors and photonic (Hammami et al., 2008). Dielectrics are a class of materials that are poor conductors of electricity, in contrast to materials such as metals that are generally good electrical conductors.

2.4 Dieletric Materials

Dielectrics are a class of materials that are poor conductors of electricity, in contrast to materials such as metals that are generally good electrical conductors. Many materials, including living organisms and most agricultural products, conduct electric currents to some degree, but are still classified as dielectrics. The electrical nature of these materials can be described by their dielectric properties, which influence the distribution of electromagnetic fields and currents in the region occupied by the materials, and which determine the behavior of the materials in electric fields (Stuart, 2010).

Dielectric material is a ceramic material that good in electrical insulators which do not contain free charges for conduction. A dielectric material is a substance that is

a poor conductor of electricity, but an efficient supporter of electrostatic fields. Dielectrics contain positive and negative charges which are bounded together and these charges could be effected by the electric field. The main function of dielectric is the charge storage. This property is very useful in capacitors, especially at radio frequencies. There are many examples of dielectric material such as NiO, Calcium Copper Titanium Oxide (CCTO) and Fused Silica (SiO_2). In this study, the focused subject was NiO as the host material doped with TiO_2 as the dopant.

2.5 NiO

Based on the literature, there are many general and specific characteristics of NiO were stated. NiO is a well-known antiferromagnetic material (Fujii, 1996). It has a versatile wide band gap semiconductor material (Venter & Botha, 2011). NiO finds a wide range of applications due to its good chemical stability as well as excellent optical and electrical properties. NiO is a semitransparent p-type semiconducting material with band gap width of about 3.8 eV (Lei et al., 2008). It shows attractive electric, electrochromic and thermoelectric properties as well as high chemical resistance (Hotový et al., 1998; Azens, 1998; Shin et al., 2000). NiO is being considered as one of the promising potential electrode materials for supercapacitors as well as for many other applications such as catalyst, electrochromic films, p-type transparent film and fuel cell electrodes (Aswal & Gupta, 2007).

In this study, NiO acted as the hosted materials that doped with TiO_2. The previous study reported the (Li, Ti)-doped NiO prepared by the sol–gel method has giant dielectric constant ($<10^5$) near room temperature in low frequency. They found that the Ti content had a remarkable effect upon the microstructure and dielectric

constant of LTNO. With increasing of Ti concentration, grain size changing and the dielectric constant variety were observed (Nan et al., 2002).

Others, the electrical properties of (Li, Al)-doped NiO ceramics (i.e., $Li_{0.05}Al_{0.04}Ni_{0.91}O$, $Li_{0.05}Al_{0.06}Ni_{0.89}O$, and $Li_{0.05}Al_{0.10}Ni_{0.85}O$) synthesized by a simple thermal decomposition route were investigated. It was observed that the grain size of the ceramics was affected by the Al content. Impedance analysis confirmed that these ceramics had an electrically heterogeneous structure that was responsible for the giant dielectric response. Interestingly, the Al-dopant had not only the strong effects on the electrical transport character at grain boundaries, but also on the conductivity in the grain interiors (Tangwancharoen et al., 2009).

2.6 TiO_2 as a Dopant

Ti is very useful as dopant in increasing dielectric properties when it was doped into glasses, NiO and Fe. Li and Ti co-doped NiO thin films with 200 nm in thickness were deposited onto Pt/Ti/SiO_2/Si (100) substrates using a sol-gel spin-coating method. The effect of Ti doping content on microstructure and dielectric properties of $Li_{0.10}Ti_xNi_{(0.90-x)}O$ (x = 5-20 mol %) thin films was investigated. XRD results showed that all the $Li_{0.10}Ti_xNi_{(0.90-x)}O$ thin films consisted of a mixture of NiO, Li_2NiO_2 and $NiTiO_3$ oxides. The intensities of the diffraction peaks for the $NiTiO_3$ phase increased and those for NiO decreased with increasing Ti content, suggesting that a part of NiO phase combined with Ti to form $NiTiO_3$ phase. The dielectric constants of all the $Li_{0.10}Ti_xNi_{(0.90-x)}O$ thin films at 102 Hz at room temperature ranged from 200 to 400 and increased with increasing Ti content. The frequency stability of the dielectric

constant for the $Li_{0.10}Ti_xNi_{(0.90-x)}O$ thin films was also improved greatly with increasing Ti content (Zhang et al., 2007).

Other reported research that the polycrystalline $GaFe_{(1-x)}Ti_xO_3$ (x = 0, 0.05, 0.10, 0.15 mol %) samples were synthesized by solid state reaction. The effect of substitution of Ti at the Fe site on the structural parameters, dielectric and magnetic was studied. The monophasic compounds crystallized in the orthorhombic space group pc21n and the unit cell volume decreases with increasing Ti content. The dielectric constant has increased while the dielectric loss has decreased at higher temperature as compared to parent compound $GaFeO_3$ after doping Ti ions at the Fe site. Doping of Ti has also decreased the ferrimagnetism (Sen, 2016).

Basically, through the previous study, TiO_2 as dopant in electroceramics can improve the dielectric properties of those electroceramic materials. Thus, the effect of doping various amount of TiO_2 into NiO was studied. The experimental work that had been done was using the solid-state method to synthesis and characterize the undoped and TiO_2 doped NiO in order to decrease the dielectric loss, improve the dielectric constant and density of NiO.

2.7 Solid-State Method

NiO needs to be synthesis even it is a good insulator because this material's characteristics can be improved time by time. This study provides a simple method which is solid-state method to synthesis and characterize NiO.

Solid state reaction route is the most widely used method for the preparation of polycrystalline solids from a mixture of solid starting materials. Solids do not react together at room temperature over normal time scales and it is necessary to heat them

to much higher temperatures, often to 1000 °C to 1500 °C in order for the reaction to occur at an appreciable rate. The factors on which the feasibility and rate of a solid-state reaction include, reaction conditions, structural properties of the reactants, surface area of the solids, their reactivity and the thermodynamic free energy change associated with the reaction (Viruthagiri et al., 2013).

Through the solid-state method, NiO need to be highly pure, be a fine powder and be a large single crystal. This method consists of heating two non-volatile solids which react to form the required product. It also can be used to prepare a whole range of materials and an extremely large number of compounds. However, in this experimental work, there were basic processes such as ball milling, calcination, pellet shaping and sintering processes before the further tests.

2.7.1 Ball Milling Process

Ceramic materials can be produces either indirectly or directly via ball milling (ˇSepelák et al., 2012). Furthermore, ceramics can be incorporated into different matrices by ball milling, so to enhance mechanical properties (Hussain et al., 1996).

Grinding occurs by impact among the milling media (balls and jars), driven by centrifugal and Coriolis forces, with material particles typically covering balls and/or jar surfaces. The energy available for comminution and, in turn, the size of the ground particles and their defectivity, are determined by several parameters, related both to geometry and to physical properties of jar and milling media. These include size and shape of balls and jar, elastoplastic properties and friction coefficients, but also angular velocities, grinding time and charge fraction. Products homogeneity and

contamination from the vials are also related to the above-defined parameters and must be properly accounted for (Broseghini et al., 2016).

Next, after the powder samples done for ball milling process, there are calcination process for this experimental work.

2.7.2 Calcination Process

The calcination process is generally carried out at a temperature lower than the melting point of the calcinated product (Ciesielczyk et al., 2014). In various research papers the influence of calcination on the physicochemical properties of oxide materials was described so far. Selection of the calcination process parameters of the powder is important from the point of view of porous structure, hydrophilic hydrophobic nature, crystalline structure and dispersion characteristics (Ibrahim, 2012; Ren, 2013; Saruchi, 2013).

Calcination process is gaining importance in area of today's technology, giving the ability to control the physicochemical properties of calcinates (moisture content, sorption capacity, diameter and pore volume, surface activity, the hydrophilic hydrophobic character), resulting in subsequent directions of their use, despite various costly modifications with other compounds (Ciesielczyk et al., 2014). After the calcination process, the powder was grinded and sieved to be finer powder. Then, it was ready for shaping process.

2.7.3 Shaping Process

Cold compaction is the first step in giving shape to powders in PM processes. There are different methods of cold compaction, such as uni-axial pressing, cold isostatic pressing, bi-axial and tri-axial pressing, metal injection molding, explosive compaction and hydrostatic pressing (Verlinden & Froyen, 1995). However, uni-axial pressing is the simplest and most widely used process for preparation of green compacts.

Based on Verlinden & Froyen (1995), the step of preparation of green compact is shown in Figure 2.1. In stage 1, the particles get re-arranged with substantial increase in green density. In stage 2, which begins at higher pressure, individual particles are deformed and in stage 3, cold welding occurs between particles providing dimensional stability and green strength required for easy handling and further processing.

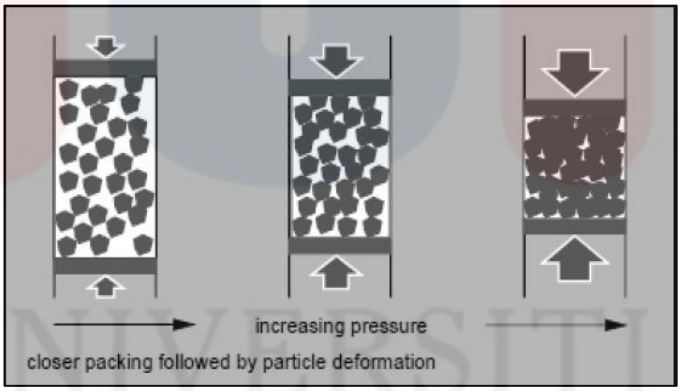

Figure 2.1: Steps in preparation of green compact

Green compacts can be prepared with or without binders depending on the composition of the elemental powders and subsequent sintering process. Higher green strength results in more robust handling of green parts prior to the sintering operation and reduced levels of green scrap. In this experimental work, after the compaction process of powder to be pellet shape, those pellets were done for sintering process.

2.7.4 Sintering Process

Sintering is a diffusional process that proceeds at relatively high temperatures, usually between 1/2 or 3/4 of the melting temperature of the ceramic (Barsoum, 1997). During sintering, material is transported to inter-particle necks to build a strong ceramic bond. The purpose of the sintering step is to convert a porous powder compact into a useful part. For a few ceramics such as porous insulating refractories, this means vapor phase transport of material that builds strong necks without a significant increase in bulk density (Kingery et al., 1976).

In contrast, Barsoum (1997) stated that that many ceramics undergo a significant increase in density during sintering that is crucial for developing desirable properties such as mechanical strength, optical translucency, or dielectric constant. Example of the neck-growth during non-densifying and densifying sintering was shown in Figure 2.2. This explained that the sintering process could increase the density of ceramic besides improving many of desirable properties. The sintering process could bring the neck-growth of compacted powder and make it denser.

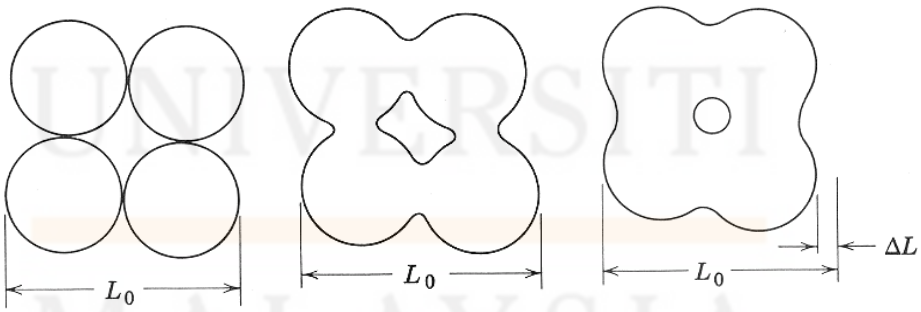

Figure 2.2: Schematic representation of (a) a powder compact, (b) non-densifying neck-growth, and (c) densifying neck-growth

In conclusion, the aim of this study is to obtain the dielectric performance, density, phase formation and microstructure of NiO via conventional ceramic solid-state reaction method using TiO_2 as dopant.

CHAPTER 3

METHODOLOGY

3.1 Introduction

This research is focus on the study of the effect of different amount of TiO_2 doped into NiO dielectric material. Several tests have been done such as X-Ray Diffraction (XRD), Scanning Electron Microscopy (SEM), density and dielectric testing to investigate the effectiveness of TiO_2 as dopant on the NiO properties. The sample preparation and testing methods will be discussing more details in this chapter.

3.2 Starting Materials

In this section, the details on the raw materials used which are NiO powder and TiO_2 powder, includes of their functions in this solid-state reaction of this study. Table 3.1 shows the information of the materials used in this experiment.

Table 3.1: Raw material that have been used in TiO_2 doped into NiO

Materials	Colour	Purity (%)	Function
NiO	Green	99.9	Host material
TiO_2	White	99.9	Dopant- to increase the dielectric constant, decrease dielectric loss and densification

3.3 Experimental Designs

The aim of this experiment was to produce $Ni_{1-x}Ti_xO_{1+x}$, with the improvement of dielectric properties. This experiment is on $Ni_{1-x}Ti_xO_{1+x}$ ceramics where the dopants concentration was emphasized. The $Ni_{1-x}Ti_xO_{1+x}$ ceramics were prepared and synthesized by using solid-state reaction method.

The formula for $Ni_{1-x}Ti_xO_{1+x}$ is referred to the ratio of NiO and TiO_2 powder content in the sample mixtures. The whole ratio is 1 and 1-*x* is the total of NiO content. *x* is replaced by the amount of TiO_2 in the compound according to the composition stated which are 0, 0.01, 0.02, 0.03, 0.05 and 0.10 mol %.

The raw materials were wet mixed with ethanol as wet medium for 24 hours using zirconia ball as the mixing medium. The time taken for mixing process was enough to allow the samples mixed well. Then, the mixture powder was calcined at 950 ºC for 4 hours using the furnace. The heating and cooling rate is 5 °C/min.

Next, the mixture powders were grounded using agate mortar to be finer powder. The calcined powders were compacted into pellets with 6 mm diameter using the hydraulic hand press machine of 250 MPa. Next, the sintering process was done at 1250 ºC for 5 hours using furnace with heating and cooling rate of 5 ºC/min. Table 3.2 shows the parameter used in this experiment.

Table 3.2: The parameters in $Ni_{1-x}Ti_xO_{1+x}$ synthesis

Parameters	Descriptions
Method	Solid State Reaction
Amount of TiO_2 mol %	0, 0.01, 0.02, 0.03, 0.05, 0.10 mol %
Calcination	Temperature: 950ºC Durations: 4 hours
Shaping	Pressure: 250 MPa Size: 6 mm
Sintering	Temperature: 1250ºC Durations: 5 hours

Characterization and analysis of the sample were carried out by using XRD for structural analysis, SEM for microstructure analysis, density by Archimedes principle and dielectric measurement by using impedance analyzer. Figure 3.1 shows the process flow of this experimental work.

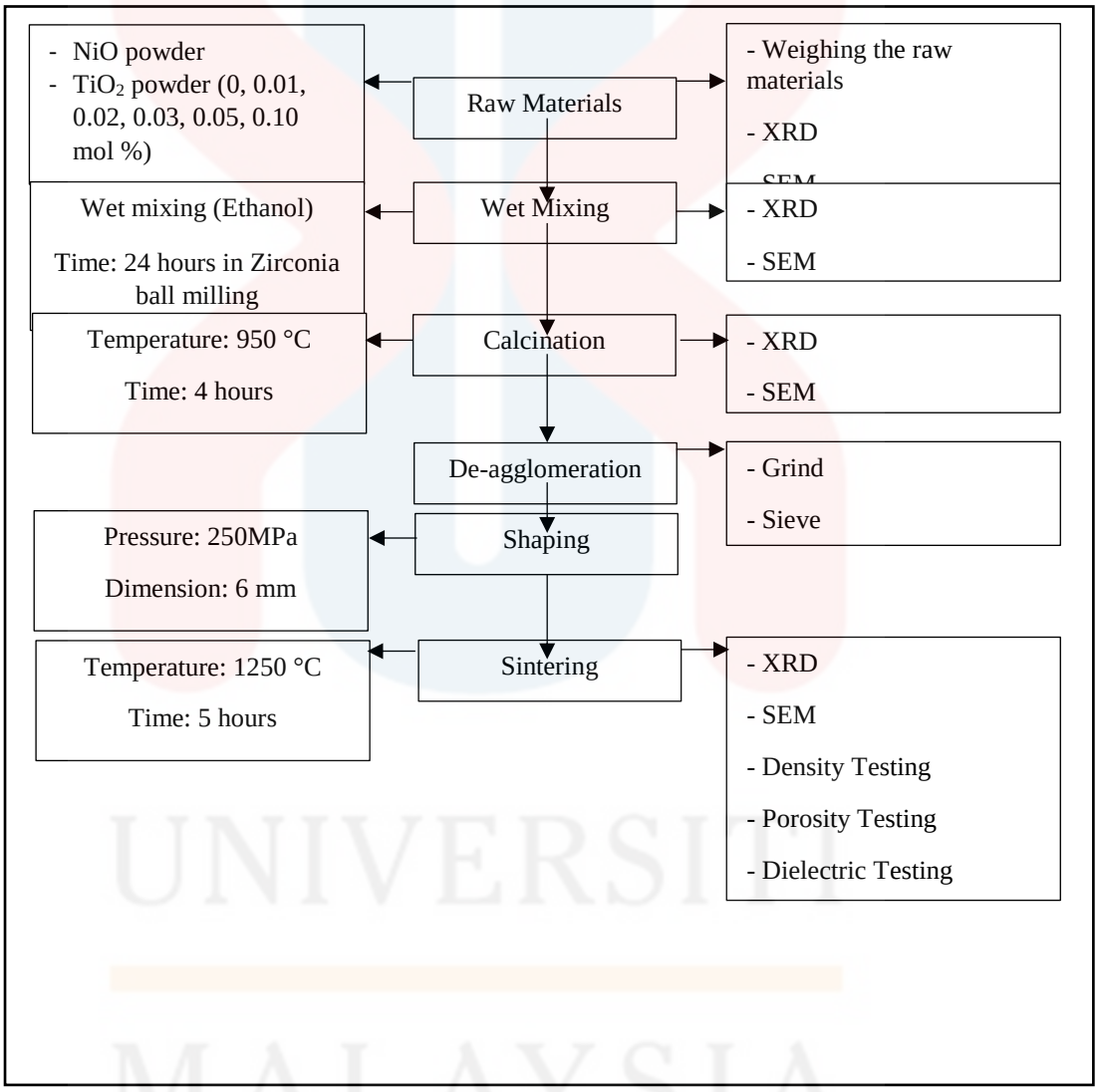

Figure 3.1: The process flow of experimental work

3.4 Processing Steps

This section of processing step is about the further details for every processing step throughout this experimental work.

3.4.1 Calculation of Stoichiometric Composition and Weighing Process of Raw Materials Needed

The $Ni_{1-x}Ti_xO_{1+x}$ was weighed based on the stoichiometric formula as shown in Equation (3.1). The raw materials were weighed by using digital weight balance that is set into four decimal places to get an accurate reading and for ease weight measurement.

$$(1-x)\ NiO + x\ TiO_2 \rightarrow Ni_{1-x}Ti_xO_{1+x} \quad (3.1)$$

The mass of raw material needed for NiO and TiO_2 can be calculate based on the Equation (3.1). The total mass of raw materials from each sample is 12 g. For example, based on Equation (3.1), $Ni_{1-x}Ti_xO_{1+x}$ can be obtained. When x = 0.01, the chemical reaction is as shown in Equation (3.2):

$$0.99NiO + 0.01TiO_2 \rightarrow Ni_{0.99}Ti_{0.01}O_{1.01} \quad (3.2)$$

Hence,

Mole of $Ni_{0.99}Ti_{0.01}O_{1.01}$ = Total mass of raw materials / (Total molar mass of $Ni_{0.99}Ti_{0.01}O_{1.01}$ x Number of mole)

= 12 g / [(58.6934 x 0.99 mol) + (43.867 x 0.01 mol) + (15.9994 x 1.01 mol)]

= 0.1605468654 g/mol

There is 1 mol of $Ni_{0.99}Ti_{0.01}O_{1.01}$ = 1 mol of NiO + 1 mol of TiO_2.

Thus, the mass of raw materials used can be calculated as below:

Mass of NiO = [Mole of $Ni_{0.99}Ti_{0.01}O_{1.01}$ x Total of molar mass of NiO] x Number of mole of NiO

= [0.1605468654 g/mol x (58.6934 + 15.9994 mol)] x 0.99

= 11.8718 g

Mass of TiO_2 = [Mole of $Ni_{0.99}Ti_{0.01}O_{1.01}$ x Total of molar mass of TiO_2] x Number of mole of TiO_2

= [0.1605468654 g/mol x (43.867 + 2(15.9994) mol)] x 0.01

= 0.1282 g

For 1 mole % of $Ni_{0.99}Ti_{0.01}O_{1.01}$ sample preparation, 0.1282 g of TiO_2 was used to dope 11.8718 g of NiO. Table 3.3 shows the composition for raw materials that were used in the preparation of $Ni_{1-x}Ti_xO_{1+x}$.

Table 3.3: Composition of raw materials used in $Ni_{1-x}Ti_xO_{1+x}$ sample preparation

$Ni_{1-x}Ti_xO_{1+x}$	**TiO_2 used (g)**	**NiO used (g)**
x = 0	0.0000	12.0000
x = 0.01	0.1282	11.8718
x = 0.02	0.2563	11.7437
x = 0.03	0.3841	11.6159
x = 0.05	0.6394	11.3606
x = 0.10	1.2743	10.7257

3.4.2 Mixing

After weighed the raw materials based on its compositions, the mixing process for those compositions were needed. Mixing process is one of the method used in this experiment works which used for chemical and physical uniformity improvement of the mixture. By using ball mill as the mixing process, the mixture can mix properly. Ball mill is a type of grinder used to grind and blend materials especially the powder

mixture. The size of particles will reduce by impact as the balls drop from near the top of the shell. Figure 3.2 shows the schematic diagram of working principle of ball mill process.

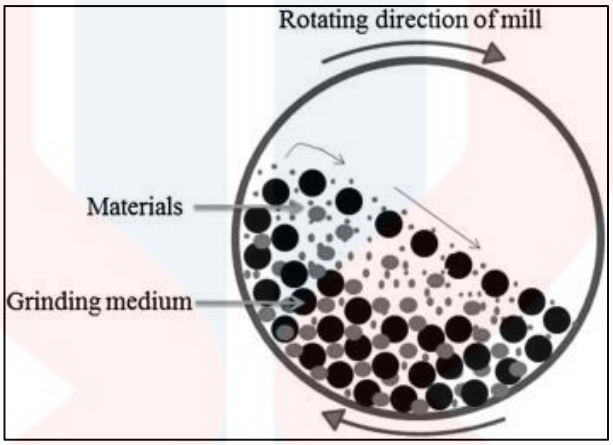

Figure 3.2: Schematic diagram of ball mill working principle

Zirconia balls are used in this experimental work because of its properties of the hardness is able to reduce the wear that will occur in milling process. This process also can reduce the impurities that present in the raw materials. The weight of zirconia balls used for every sample was calculated by using the ratio of 1:10.

Weight of zirconia balls = Weight of sample x 10

= 12 g x 10

= 120 g

When the mass of raw materials is 12 g, thus the weight of zirconia balls used in this experimental work is 120 g for every sample.

Ethanol was used as the medium in the wet mixing process. The amount of ethanol used for every sample is based on the weight of sample too. The weight of ethanol used for this experiment is 2 % of sample weight.

Amount of ethanol = 2 % x 12 g

= (2/100) x 12 g

= 0.24 g

Thus, 0.24 g of ethanol is used as the mixing medium for 12 g sample.

Then, the mixture was put into the milling machine for 24 hours to ensure the mixture mixed well. After that, the sample was dried for the further steps of experimental work which was calcination.

3.4.3 Calcination

Calcination is a process of subjecting a substance to the action of heat in high temperature, but below melting point, for the purpose of causing loss of moisture, reduction or oxidation, and dissociation into simpler substances.

In this experimental work, alumina crucible was used as the container for calcination process due to its good properties that can withstand in high temperature up to 1750 °C, durable and inert to any chemicals. Before the calcination process, the crucible is need to clean up to avoid any contamination and put into the oven with temperature of 100 °C for 10 minutes to dry completely. Figure 3.3 shows the alumina crucibles used in this experimental work.

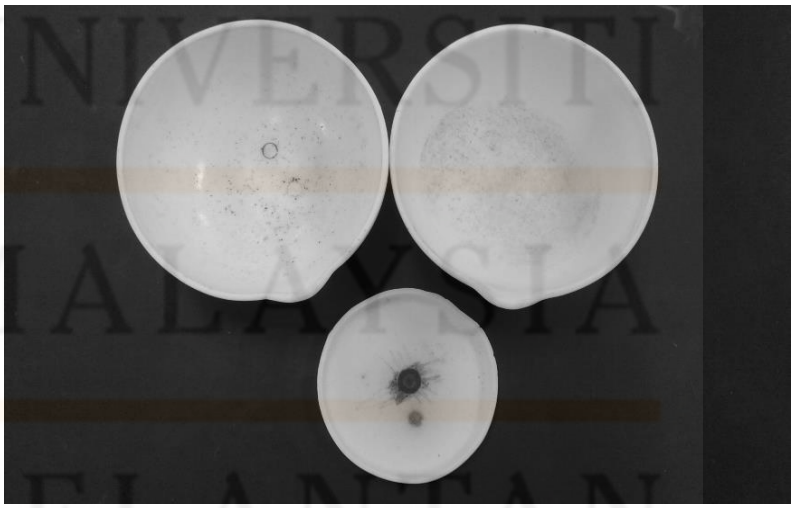

Figure 3.3: Alumina crucibles used in this experimental work

The mixture was placed into the crucible and placed in a high temperature furnace. The calcination temperature in this study was 950 °C for 4 hours, while the heating rate and cooling rate were 5 °C/min. Then, the calcined powder was ready for de-agglomeration process. Figure 3.4 shows the graph of temperature changes throughout the calcination process.

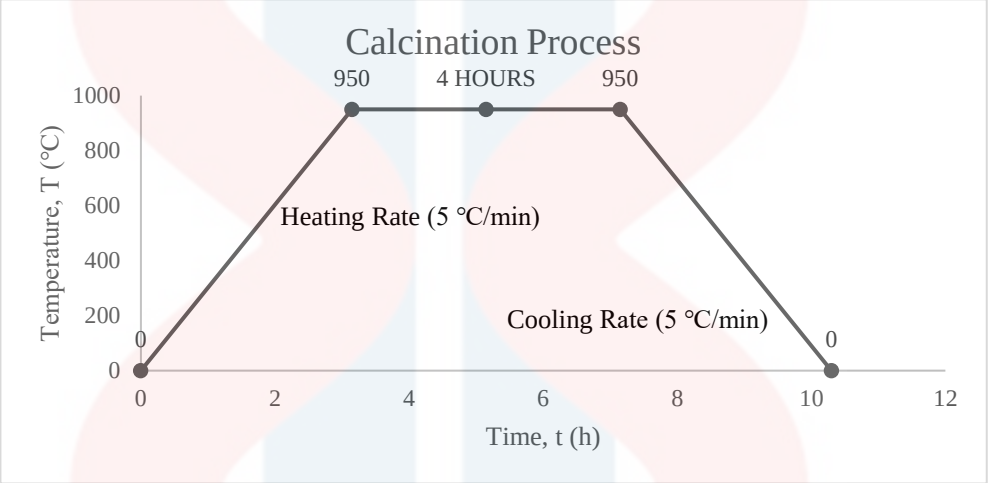

Figure 3.4: The graph of temperature against time in the calcination process

3.4.4 De-agglomeration

The de-agglomeration process is very important step after the calcination process. The calcined powders usually agglomerate and coarser compared to the raw material powders. It usually occurred at the high calcined temperature and cause the powders getting hard to press into pellet form. Thus, the calcined powders were grinded and sieved by using the agate mortar as shown in Figure 3.5 to produce the finer powder. This process was done until the mixture powder mixed well and been very fine powder. After de-agglomeration process, the powders were ready for shaping into pellet form.

Figure 3.5: Agate mortar for de-agglomeration process

3.4.5 Shaping

The Specac hydraulic pressing machine as shown in Figure 3.6 was used to compact $Ni_{1-x}Ti_xO_{1+x}$ powder with 6 mm diameter cylindrical mold to produce the pellet form. The pressure applied for pellet forming was 250 MPa.

Figure 3.6: Specac Hydraulic Pressing machine used for shaping process

The mold need to be clean and free from any particles to avoid the sample contamination. SW-401 lubricant spray was used to clean the mold. The powder was weighed and poured into the mold. For 6 mm pellet, 0.1250 g of mixture powder was used to produce ~1.35 mm pellet thickness. The mold was agitated and slightly compressed with the manual forced to obtain even surface of the pellet.

The pressure was released a few times during subsequent pressing to its maximum load to remove entrapped air in the powder. The pressure then held for 2 minutes at 250 MPa to ensure the force can well distributed. Then, after the pellets were removed by using tweezer with care. Figure 3.7 shows the pellet produced in this shaping process. Next following step was sintering process.

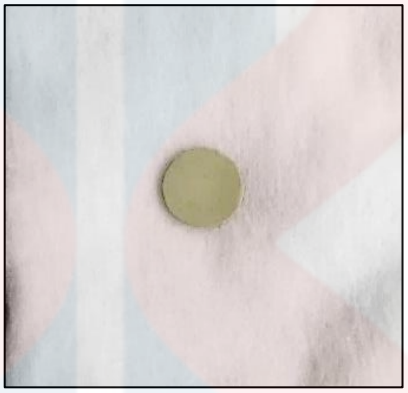

Figure 3.7: Pellet produced in shaping process

3.4.6 Sintering

Sintering is a heat treatment applied in order to impart strength and integrity. It usually used in the manufacture of pottery and ceramic objects. The pressed pellet was sintered in order to produce a dense product.

Alumina crucible was used in this process as the container and the steps taken were same as in the calcination process but with the different sintering temperature. The crucible need to clean up to avoid any contamination and put into the oven with temperature of 100 °C for 10 minutes to dry completely. The mixture was placed into the crucible and placed in a high temperature furnace with temperature of 1250 °C for 5 hours. The heating rate and cooling rate were 5 °C/min. Figure 3.8 shows the graph of temperature changes throughout the sintering process.

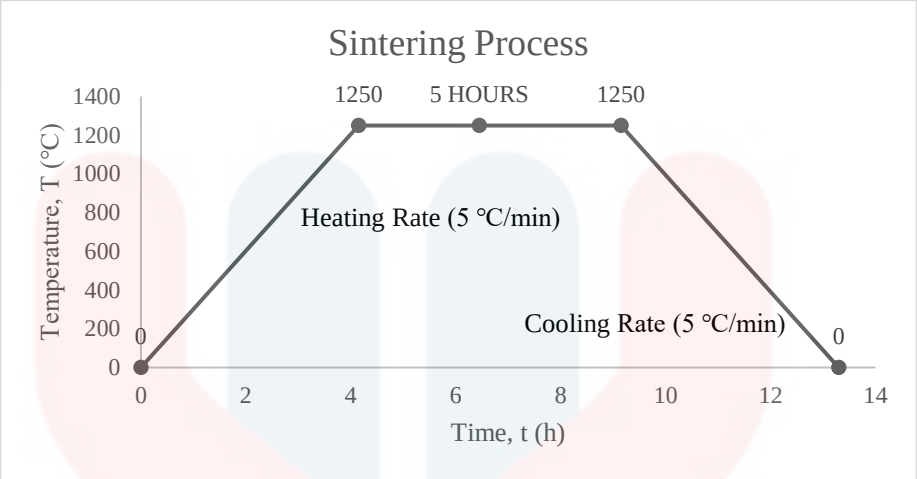

Figure 3.8: The graph of temperature against time in the sintering process

3.4.7 Characterization Method

In this experimental work, the characterization methods are very important. This method used includes XRD for phase information, SEM for surface morphology, impedance analyzer for dielectric properties and Archimedes principle for density. Each of them are needed for analyzing and characterizing steps for all compositions.

3.4.7.1 X-Ray Diffraction (XRD)

XRD is mainly used for determination and identification of any existing elements of the sample. The step for fine powder, they were mounted on the glass slit and pressed into the smooth compacted layer in the aluminium based sample holder. For the sintered pellet step, the pellet was placed directly in the sample holder and located at the center of the diffraction chamber.

The sample was exposed to CuKα radiation (λ = 1.540Å) in reflection mode and the reflection was recorded by a detector. The data have been collected by step-

scanning 2θ from 10° to 90°. Phase identification was performed by matching the sample diffraction pattern with the recognized database.

3.4.7.2 Scanning Electron Microscopy (SEM)

SEM is one of the testing machine that use to analyze morphology image of the sample. The SEM is capable of magnifying the sample's surface to 1,000,000 times of its original size. It consists of Energy Dispersive Spectroscopy and electron backscattered diffraction arrangement.

The samples are mounted on the holders or stubs using double-sided conductive tapes or silver paint for sample mounting with complete drying before loading into SEM chamber. Small pellet can be mounted directly on pore-plate.

3.4.7.3 Density Testing

One of the main purpose in this testing is the effect of dopant concentration towards the density of NiO. The sample was weighted by using RADWAG Density Kit to obtain the dry weight, D. Then, the sample was measured the saturated weight, W. The sample was placed into the stand in the water and measured its suspended weight, S. After all of the measurements obtained, the calculation was done by using Equation 3.4 and 3.5 to obtain the value of density and porosity.

In this study, the densities of the pellets were obtained by using the Archimedes principle. The bulk equation was used to calculate the density value of the pellet. The volume of pellet was determined using the water displacement when the pellet was immersed. The bulk density was obtained by using Equation 3.4.

$$\text{Bulk density, } \rho = \frac{\text{D x } \rho(\text{water})}{\text{W} - \text{S}} \quad (3.4)$$

Where,

$\rho_{(water)}$ = Density of Water (g/cm^3) = 1.00 g/cm^3

D = Dry weight, (g),

W = Saturated weight, (g),

S = Suspended weight, (g)

The apparent porosity was calculated as well using Equation 3.5 to compare the porosity percentage against different concentration of dopant.

$$\text{Apparent porosity} = \frac{\text{W}-\text{D}}{\text{W}-\text{S}} \text{ x } 100\ \% \quad (3.5)$$

Where,

D = Dry weight, (g),

W = Saturated weight, (g),

S = Suspended weight, (g)

Then, the diameter of pellet before and after sintering process is measured to calculate the shrinkage percentage. It can be calculated using the Equation 3.6 to show the shrinkage rate before and after sintering process.

$$\text{Shrinkage percentage} = \frac{\text{d1}-\text{d2}}{\text{d1}} \text{ x } 100\ \% \quad (3.6)$$

Where,

d1 = Diameter of pellet before sintering, (mm),

d2 = Diameter of pellet after sintering, (mm)

3.4.7.4 Dielectric Testing

The pellets were polished by using silicon carbide papers size 400, 600, 800, 1000, 1200 and 2000 to get flat and smooth surface of the pellets. Then, the samples were dried in the oven for 10 minutes. After that, the thickness of each pellet was measured. The surface of the pellet then swapped with silver paste to make an electrode between both of the surface to provide electrical contact between probe and the pellet.

The measurement of dielectric properties such as dielectric constant and dielectric loss was done by using impedance analyzer. The dielectric loss data was taken directly from the Impedance Analyzer. The dielectric constant value was measured by using the capacitance data and calculated by using Equation 3.7:

$$\varepsilon = \frac{Ct}{A\varepsilon_{\circ}} \tag{3.7}$$

Where,

C = Capacitance, (F),

t = Pellet thickness, (mm),

A = Silver paste area, (m^2),

$\varepsilon_{\circ}$ = Permittivity of free space taken as 8.8543 x 10^{-12} F/m

CHAPTER 4

RESULTS AND DISCUSSION

4.1 Introduction

This chapter contains the details of the analysis and the results that was obtained from the experimental works. The first section begins with the characterization of the raw materials, which are NiO and TiO_2. Then, the next section shows the result of phase formation, surface morphology, density and dielectric properties of NiO ceramics doped with different mole % of TiO_2. The effect of different concentration of TiO_2 doped into NiO properties are discussed in this chapter.

4.2 Raw Materials Characterization

Raw materials characterization is an important early stage in this study. The starting raw materials had been characterized to make the confirmation of their characteristics, especially their purity (> 99.9 %). This purity conformity is very important to ensure the finish product production in a good quality because any impurities inside the raw materials will affect the experiment results. NiO and TiO_2 had been used as the raw materials in this research.

4.2.1 NiO Powder

In this research, NiO is the green powder with 99.9 % purity as the main raw material. This powder was tested with XRD to analyze its purity. The result was plotted in Figure 4.1. Eva Software from Bruker was used to analyze the raw material's pattern. The result shows the NiO powder peaks are similar to COD file 9013980 ($Ni_{0.995}O$, bunsenite).

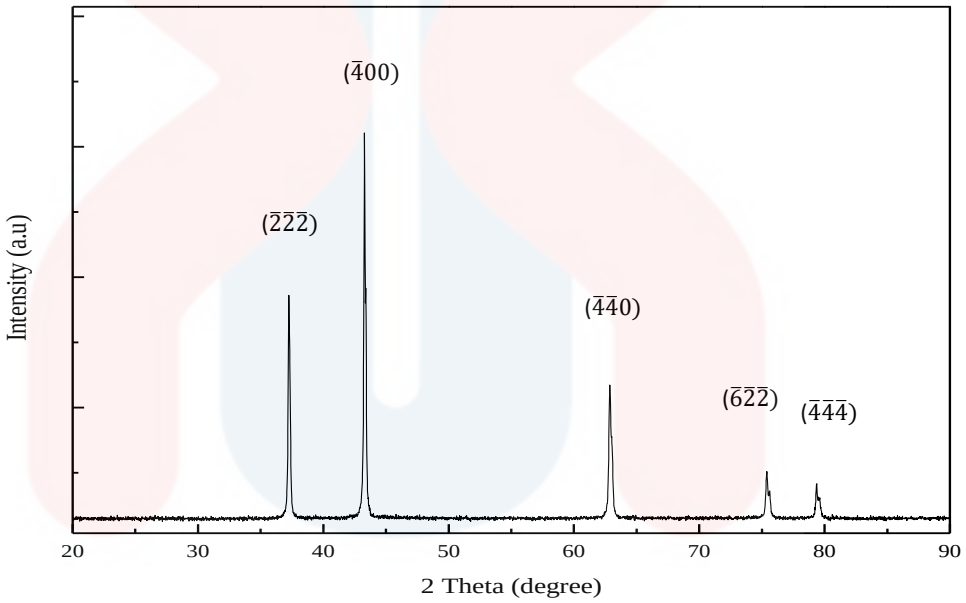

Figure 4.1: XRD pattern of NiO powder (COD 9013980 ($Ni_{0.995}O$, bunsenite))

The result shows that 2θ peaks 37.258°, 43.291°, 62.884°, 75.423° and 79.417° are indexed as $(\bar{2}\bar{2}\bar{2})$, $(\bar{4}00)$, $(\bar{4}\bar{4}0)$, $(\bar{6}\bar{2}\bar{2})$ and $(\bar{4}\bar{4}\bar{4})$. However, Ponnusamy et al. (2015) found that the diffraction peaks at 2θ were 37.2°, 43.3°, 62.7°, 75.6° and 79.4° are indexed as (111), (200), (220), (311) and (222) planes of NiO.

4.2.2 TiO_2 Powder

TiO_2 is the white powder with 99.9 % purity as the dopant raw material. This powder was added into NiO powder with various compositions. This powder was tested with XRD to analyze its purity. The result was obtained in Figure 4.2. Similar to raw NiO powder, Eva Software from Bruker was used to analyze the powder's pattern. The result shows the TiO_2 powder peaks are similar to COD file 1010942 (O_2Ti, anatase).

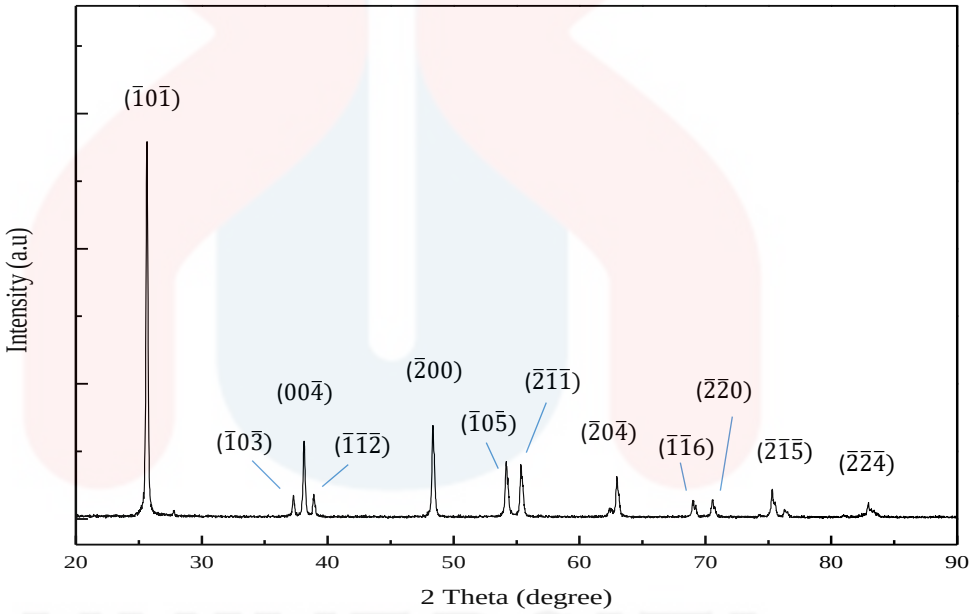

Figure 4.2: XRD pattern of TiO_2 powder (COD 1010942 (O_2Ti, anatase))

Based on Ba-Abbad et al. (2012) studies, the 2θ at peak 25.4° confirms the TiO_2 anatase structure. Besides that, Thamaphat et al. (2008) also state that the strong diffraction peaks at 25° and 48° indicating TiO_2 in the anatase phase. There is no any spurious diffraction peak found in the sample. The 2θ at peak 25.686° and 48.791° confirm its anatase structure. The intensity of XRD peaks of the sample reflects that the particles are crystalline and broad diffraction peaks indicate very small size crystallite. However, the anatase phase will transform into rutile as reported in

previous study by Yijun et al. (2002) that claimed that anatase-rutile transformation takes place in a wide of temperature.

4.3 Mixture Powder Characterization

After the raw materials were analyzed, the further steps which are milling and mixing process, calcination process, shaping and sintering process were followed by sample characterization. Those samples were labelled as in Table 4.1.

Table 4.1: Sample labelling

Composition	Label
NiO	Sample 1
$Ni_{0.99}Ti_{0.01}O_{1.01}$	Sample 2
$Ni_{0.98}Ti_{0.02}O_{1.02}$	Sample 3
$Ni_{0.97}Ti_{0.03}O_{1.03}$	Sample 4
$Ni_{0.95}Ti_{0.05}O_{1.05}$	Sample 5
$Ni_{0.90}Ti_{0.10}O_{1.10}$	Sample 6

4.3.1 Mixed Powder Characterization

Milling and mixing powder process is the early stage of this experimental work. This process was used the zirconia ball and ethanol as the mixing medium for 24 hours. This process was done to get the homogeneous mixture powder. The mixture powder gave lighter green colour than the raw NiO powder because they had been added with white TiO_2 powder. Then, they were characterized using XRD. The pattern number of these mixing powder are COD 4329323 (Ni O) and COD 9008749 (O Ti). Then, the graph of the results was plotted in Figure 4.3.

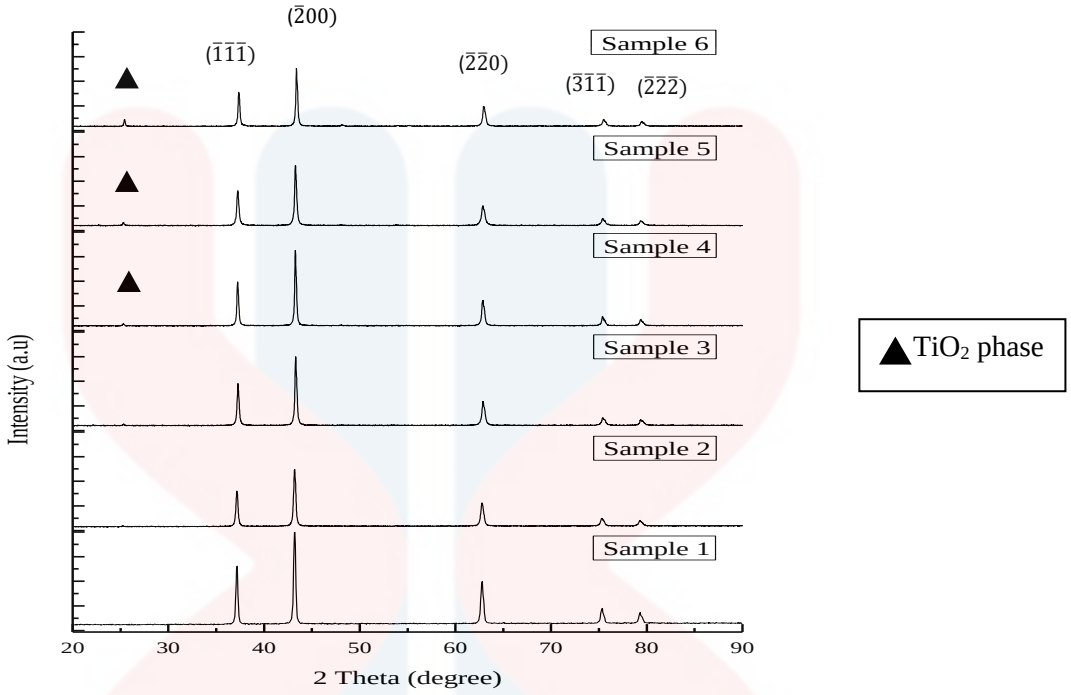

Figure 4.3: Mixed powder XRD pattern (COD 4329323 (Ni O) and COD 9008749 (O Ti))

From Figure 4.3, the calcined powder shows that there are five peaks that closely matched with the standard diffraction pattern NiO. The peaks are identified as NiO with Miller Indices of $(\bar{1}\bar{1}\bar{1})$, $(\bar{2}00)$, $(\bar{2}\bar{2}0)$, $(\bar{3}\bar{1}\bar{1})$ and $(\bar{2}\bar{2}\bar{2})$. However, in the Sample 4, 5 and 6, there are small peak at the 2θ peak 25° that signed with triangle sign. The peak higher as the concentration of TiO_2 content higher.

4.3.2 Calcined Powder Characterization

After the mixing process, the powder was calcined with temperature 950 ℃ for 4 hours. Each sample were slightly hardened during this process. However, the powder was de-agglomerated by using agate mortar and been characterized using XRD. The pattern numbers remain the same with mixed powder, which are COD 4329323 (Ni O) and COD 9008749 (O Ti). Then, the graph of the results was plotted in Figure 4.4.

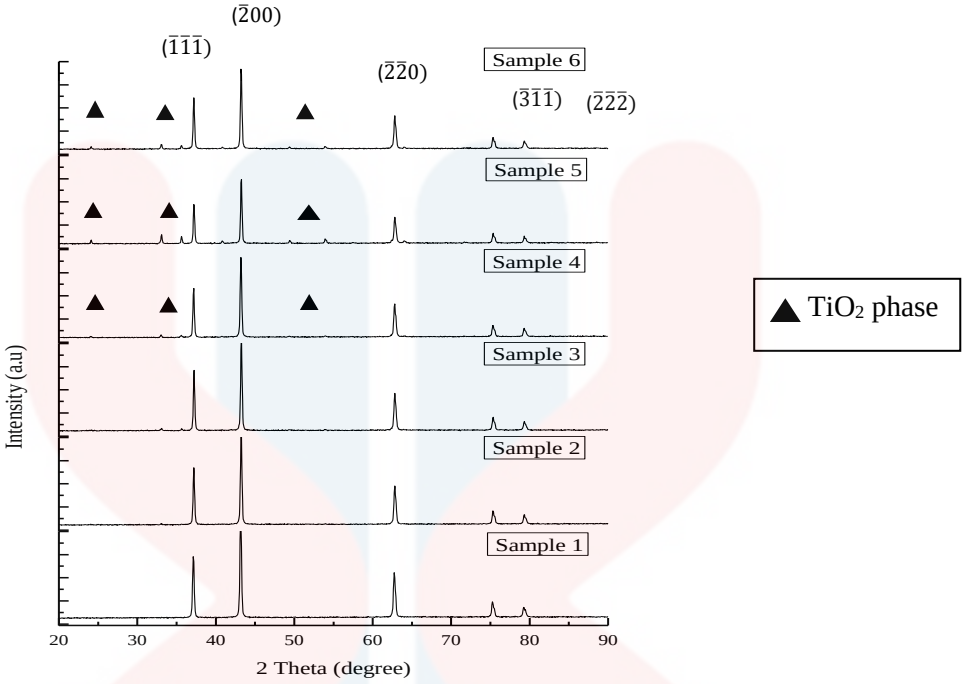

Figure 4.4: Calcined powder XRD pattern (COD 4329323 (Ni O) and COD 9008749 (O Ti))

Similar to mixed powder analysis, the major peaks are identified as NiO with Miller Indices of $(\bar{1}\bar{1}\bar{1})$, $(\bar{2}00)$, $(\bar{2}\bar{2}0)$, $(\bar{3}\bar{1}\bar{1})$ and $(\bar{2}\bar{2}\bar{2})$. The TiO_2 phase in Sample 5 is the highest intensity compared to other samples. Based on the previous study by Aliahamad et al. (2014) that studied on synthesis of Cu doped NiO, they got unchanged XRD peak pattern for every doping composition for the calcined powder, unless for their peak intensity values.

4.3.3 Sintered Pellet Characterization

After calcined, the powder was compacted into pellet form with 6 mm diameter. Then, those pellets were sintered at 1250 ℃ for 5 hours and been characterized by using XRD and SEM. Then, those pellets were weighted in dry air, suspended and saturated conditions to calculate the bulk density and apparent porosity.

4.3.3.1 XRD

The pattern numbers from XRD analysis remain the same with mixed and calcined powder which are COD 4329323 (Ni O) and COD 9008749 (O Ti). Then, the graph of the results was plotted in Figure 4.5.

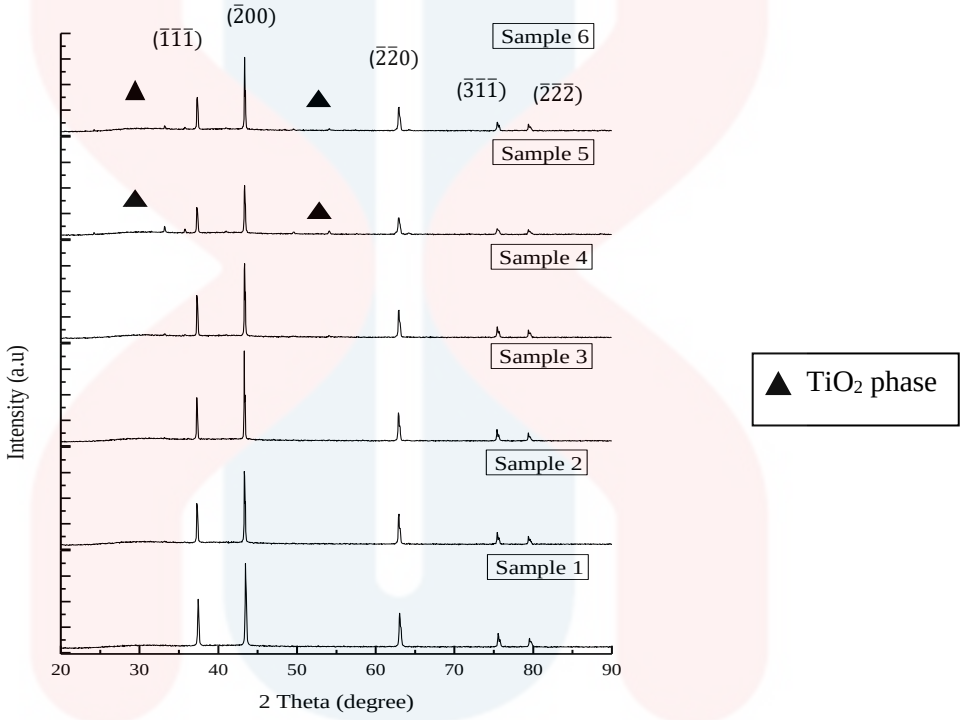

Figure 4.5: Sintered pellet XRD pattern (COD 4329323 (Ni O) and COD 9008749 (O Ti))

After sintering process, the TiO_2 reduced its intensity due to the heat treatment in sintering process caused the larger grain formation. Besides that, the graph in Figure 4.5 shows that the addition of TiO_2 up to 0.02 mole % did not change the crystal structure. The TiO_2 phase only can be seen in Sample 5 and 6 after sintering process may be due to excess TiO_2 in the crystal structure. Figure 4.6 shows the difference in peak intensity for Sample 4, 5 and 6 before and after sintering process. Sample 5 shows the TiO_2 phase in this sample is the highest intensity compared to the other samples. TiO_2 phase after calcination process reduced its intensity after having the sintering process.

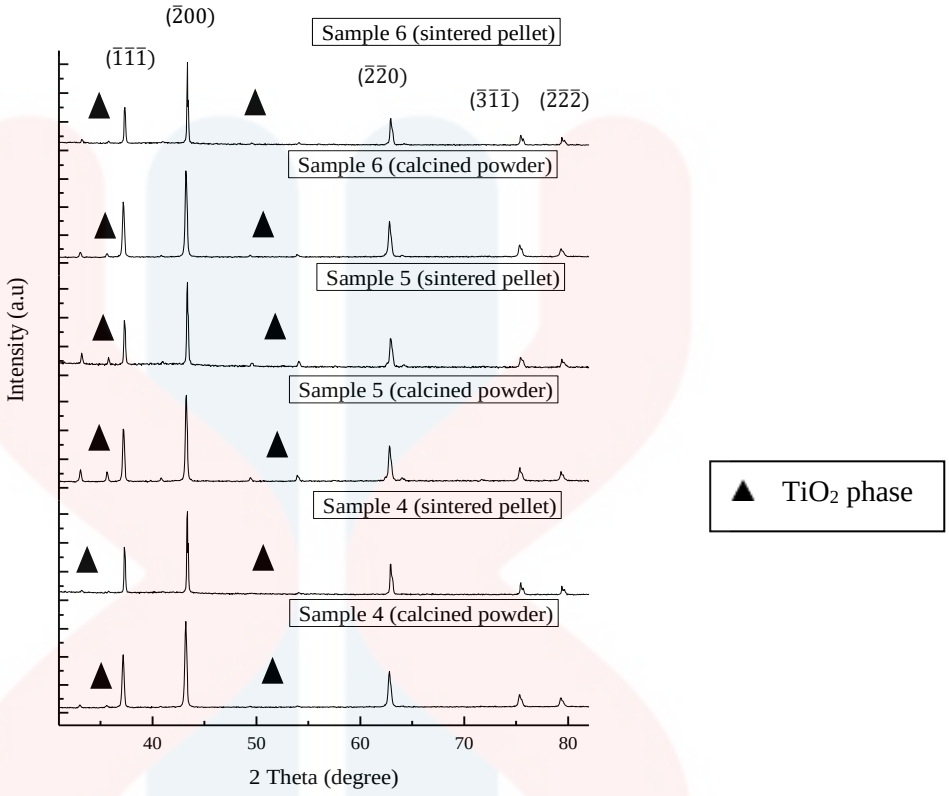

Figure 4.6: The comparison of TiO_2 phase in calcined powder and sintered pellet

Figure 4.7 shows the peaks of $Ni_{1-x}Ti_xO_{1+x}$ which correspond to the $(\bar{2}00)$. This figure shows the expanded XRD patterns corresponding to the $(\bar{2}00)$ characteristic peak. From the figure, there are NiO peaks that represented by Sample 2, 3, 4, 5 and 6. The peak shifted to the left, which means the crystallite size are getting bigger, may be due to displacement some of the Ti atom into NiO structure.

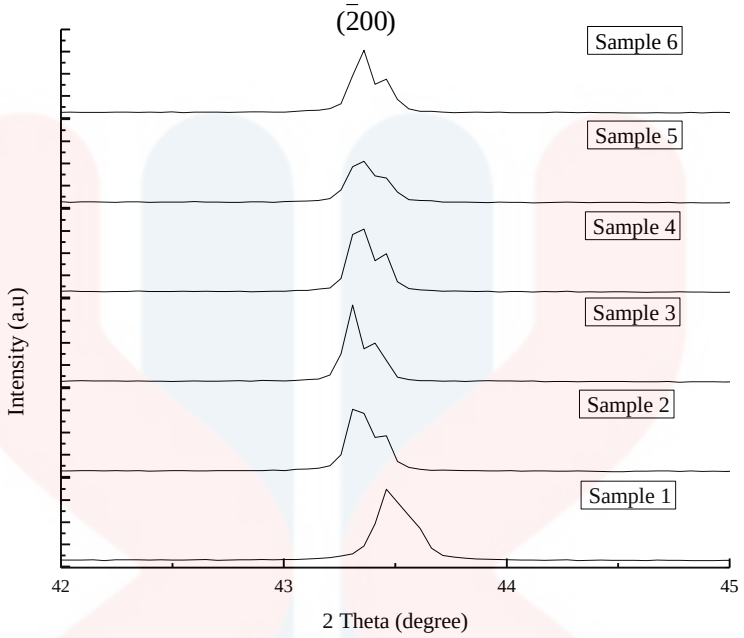

Figure 4.7: XRD patterns of sintered pellets focusing on peak ($\bar{2}00$)

Based on Liu et al. (2012) studies, they reported a different result compared to this experimental work when focused on the peak ($\bar{2}00$). They got the result of shifting of peak from low angle to high angle as the concentration of Li doped NiO increase. this might be due to smaller Li^+ atom that make the crystal shrink thus reducing the crystallite size.

4.3.3.2 Density Analysis

In this experimental work, the pellet densities were measured using Archimedes Principle. The weight of pellets had been measured using the RADWAG Density Kit in three different conditions which are dry air, suspended and saturated conditions. All conditions were measured for three times to get the accurate measurement. In this test, the bulk density and apparent porosity of each sample were calculated. Table 4.2 shows the bulk density and apparent porosity value of sample pellets.

Table 4.2: The value of bulk density and apparent porosity percentages of each sample

Sample	Composition (mole %)	Bulk Density (g/cm^3)	Apparent Porosity (%)
1	0	3.42	47.22
2	0.01	5.41	9.09
3	0.02	4.96	12.50
4	0.03	4.46	25.00
5	0.05	5.22	17.39
6	0.10	4.62	19.23

The bulk density and apparent density porosity result against different sample was plotted, as shown in Figure 4.8. Based on the overall observation in Figure 4.8, there is decrement trend for the bulk density of $Ni_{1-x}Ti_xO_{1+x}$ pellet.

Initially, the graph show increment of bulk density value from 0 to 0.01 mole %, which is from 3.42 to 5.41 g/cm^3. This is due to the addition of TiO_2 has caused densification for the $Ni_{1-x}Ti_xO_{1+x}$ microstructure, resulting in the increase of bulk density value. However, the value decrease to 4.46 g/cm^3 as the composition of TiO_2 increase to 0.03 mole %. Then, the bulk density rise to 5.22 g/cm^3 at 0.05 mole % and decrease again when 0.10 mole % of TiO_2 added with the value of bulk density is 4.62 g/cm^3. This shows that there is inconsistent value of bulk density that might be caused by the error occurred during shaping process. The pressure applied was not well distributed throughout the pellets consistently.

Besides that, Figure 4.8 also shows the apparent porosity percentage of the pellets. For pure NiO pellet, there is 47.22 % and drop to 9.09 % when 0.01 mole % of TiO_2 added into NiO. Then, the percentage increase to 25.00 % at 0.03 mole % of TiO_2. But decrease to 17.39 % at 0.05 mole % and slightly increase to 19.23 % for 0.10 mole % of TiO_2. From Figure 4.8, a relationship showed between the bulk density

value and apparent porosity percentage as the apparent porosity percentage will increase as the bulk density decrease.

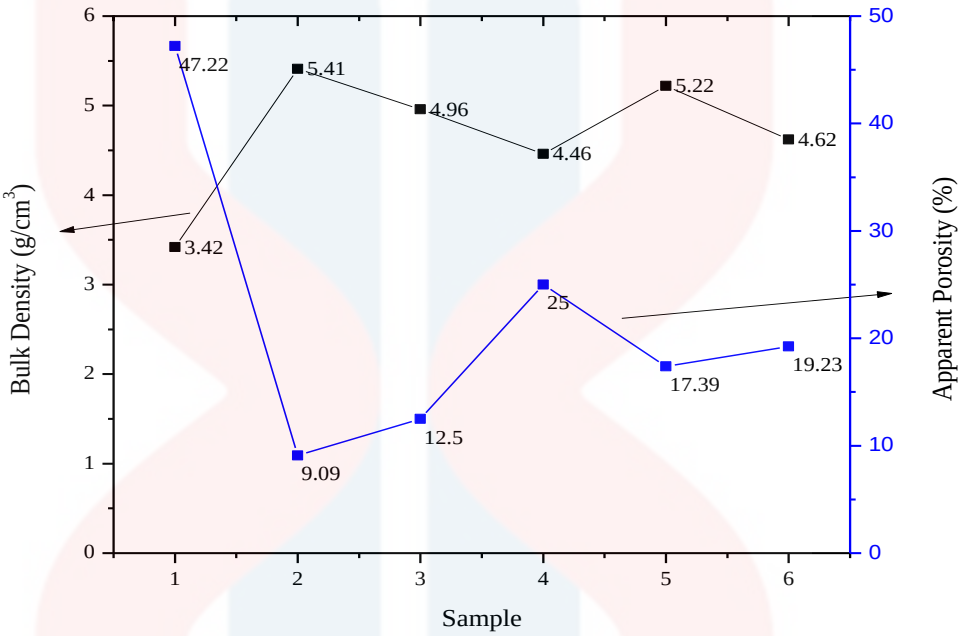

Figure 4.8: Value of bulk density and apparent porosity percentages of sintered pellets

The bulk density, apparent porosity and shrinkage rate were related to each other. To determine the shrinkage rate of $Ni_{1-x}Ti_xO_{1+x}$, diameter of pellets was measured using digital caliper before and after the sintering process. Figure 4.9 shows the $Ni_{1-x}Ti_xO_{1+x}$ measured using digital caliper. The percentage of diameter reduction was calculated and shown in Table 4.3.

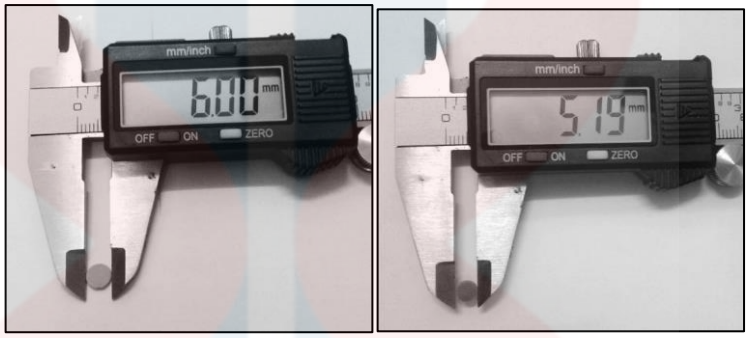

(a) (b)

Figure 4.9: The diameter measurement of pellets (a) before sintering process and (b) after sintering process

Table 4.3: The shrinkage percentage of pellets after sintering process

Sample	Shrinkage Percentages (%)
1	0.00
2	13.50
3	10.17
4	12.33
5	12.83
6	12.17

Figure 4.10 present the shrinkage rate at different dopant concentrations. It is well documented that the maximum shrinkage rate is highly dependent on the concentration of dopants (Wang et al., 2011). However, in this experimental result obtained, there is shrinkage increment from 0 % to 13.5 % when 0.01 mole % TiO_2 added into NiO. Then it decreases to 10.17 % when 0.02 mole % added and increase

to 12.83 % at 0.05 mole % added. However, the rate decreases slightly to 12.17 % when 0.10 mole % of TiO_2 added into NiO. Based on the bulk density and apparent porosity results, the shrinkage percentage is directly proportional to bulk density as the bulk density increase and the shrinkage percentage also increase, means that the apparent porosity will be decrease.

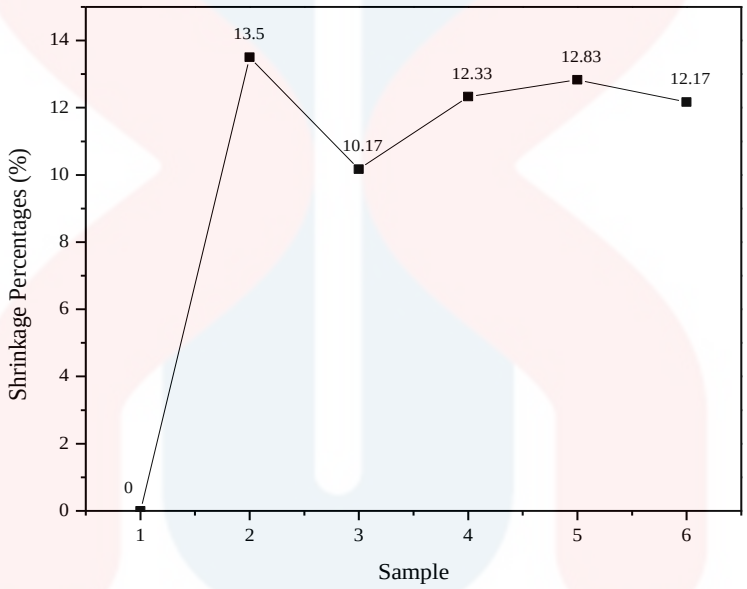

Figure 4.10: The shrinkage rate at different dopant concentration of pellet after sintering process

4.3.3.3 SEM

Figure 4.11 shows the SEM analysis of $Ni_{1-x}Ti_xO_{1+x}$ pellet after sintering process. Figure 4.11(a) shows a microstructure with a lot of pores for the undoped NiO sample. As shown in Figure 4.11, the grains distribute well as the TiO_2 content increase. The grain size increase as the TiO_2 content increase until the concentration of 0.02 mole % of TiO_2 but smaller when 0.03, 0.05 and 0.10 mole % of TiO_2 added. This shows that the 0.02 mole % of TiO_2 is the optimum TiO_2 concentration added into

NiO to get the larger grain size. However, in Figure 4.11(e) and 4.11(f), there are unknown particle shape in the pellet.

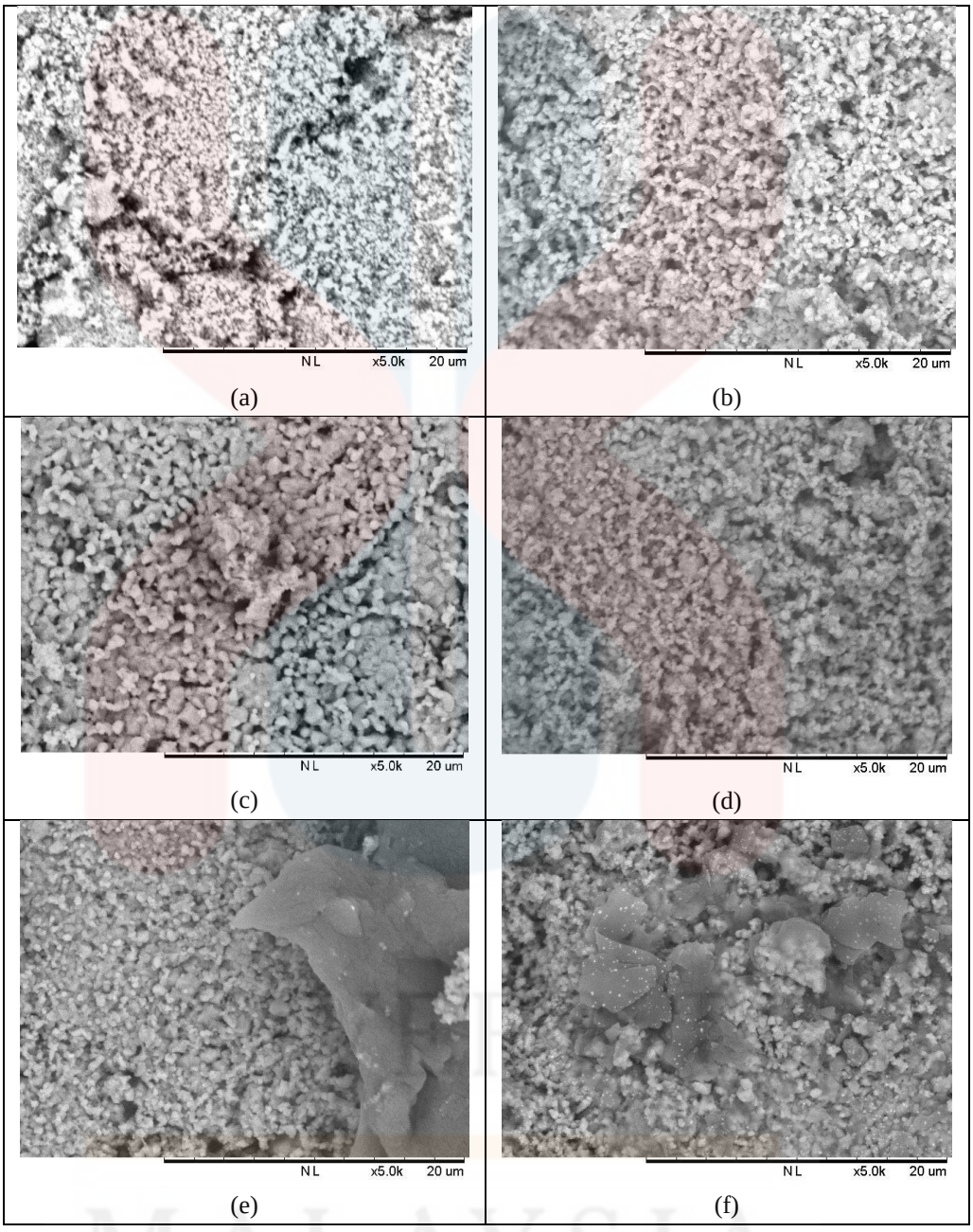

Figure 4.11: SEM microstructures of surface sintered pellets for (a) Sample 1, (b) Sample 2, (c) Sample 3, (d) Sample 4, (e) Sample 5 and (f) Sample 6

After the study of surface morphology of $Ni_{1-x}Ti_xO_{1+x}$, the sintered pellets were broken into pieces in order to examine the fracture surface morphology. Figure 4.12

shows the SEM microstructure of cross section of each sample. From the figure, it shows that the grain size bigger as the composition of TiO_2 increase.

Similar to surface morphology analysis, the grain size in Figure 4.12(c) which represent 0.02 mole % of TiO_2 is the biggest grain size compared to the other compositions. This shows that represent 0.02 mole % of TiO_2 is the optimum TiO_2 content for improving $Ni_{1-x}Ti_xO_{1+x}$ grain sizes. However, the grain sizes are quite homogenous.

Previous study by Bari et al. (2013) showed that the addition of TiO_2 nanoparticles to the LZT ceramics significantly improved the density and a dense and uniform microstructure and also abnormal grain growth were observed by SEM. The use of TiO_2 nanoparticle reduces porosity and leads to an increase in green density.

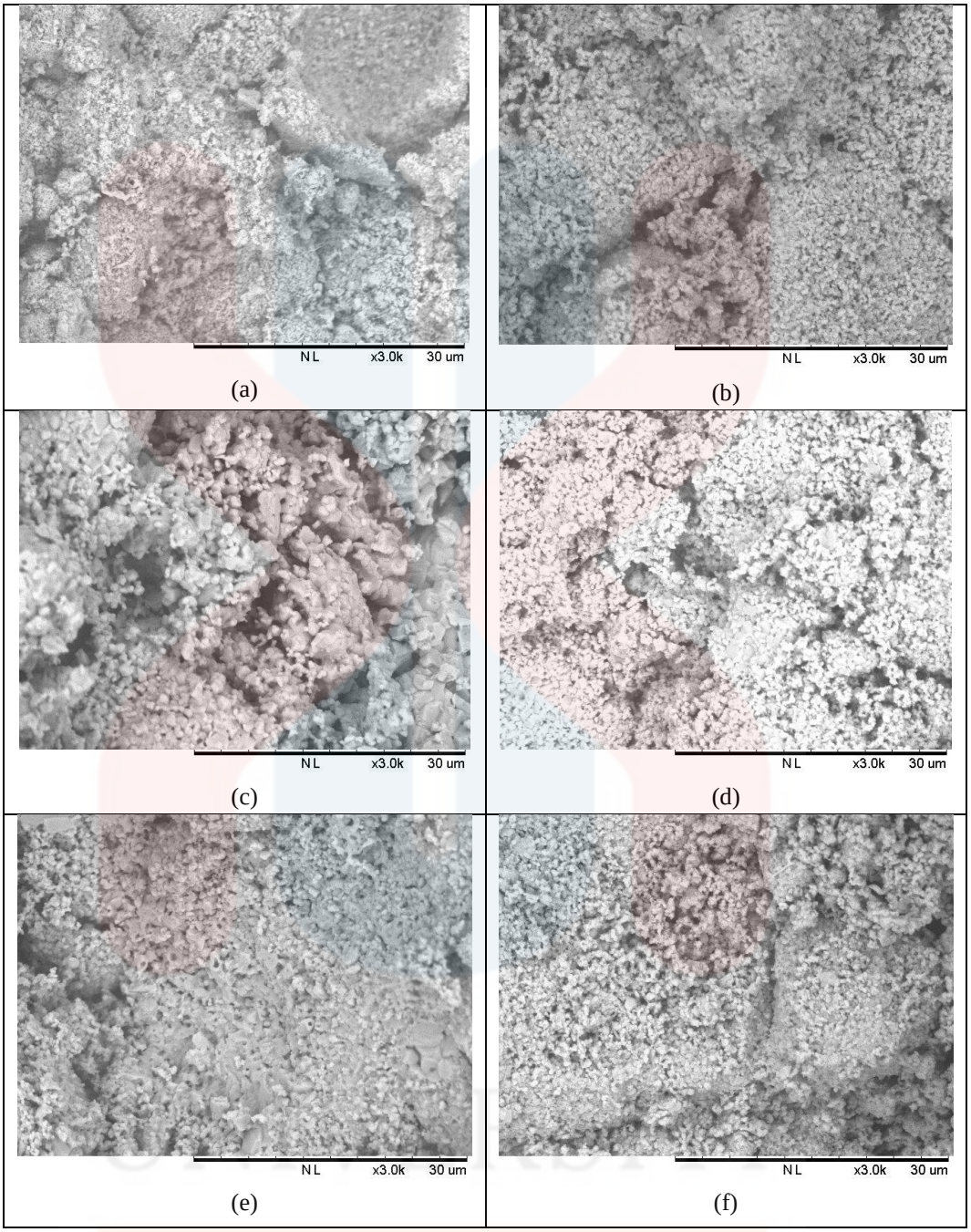

Figure 4.12: SEM microstructures of cross section surface sintered pellets for (a) Sample 1, (b) Sample 2, (c) Sample 3, (d) Sample 4, (e) Sample 5 and (f) Sample 6

4.3.3.4 Dielectric Test

The dielectric test is the most important test in this study due to the main objective of this study is to characterize the dielectric properties. The electrical properties of dielectric materials are mainly depending on dielectric constant and loss. Furthermore, the higher ε_r and lower tan δ will produce a good electroceramic product. This test is very useful in order to investigate the effect of TiO_2 dopant on the dielectric constant and dielectric loss of $Ni_{1-x}Ti_xO_{1+x}$.

Figure 4.13 shows the frequency dependence of ε_r of $Ni_{1-x}Ti_xO_{1+x}$ samples as a function of TiO_2 doping concentration. it was observed that ε_r was decreased with the increasing of the frequencies. A decrease ε_r values took place at the frequencies range between 6 – 8.25 MHz and become almost linear between 8.25 – 9.0 MHz. The ε_r was improved by the addition of TiO_2 doping. The ε_r of undoped NiO is 2.37[14] at 6 MHz, while the ε_r of 0.03 mole % TiO_2 doped NiO at gives the result of 4.51[14] dielectric constant, which is the highest value among other doping content.

This result of this study is similar to the previous study of Mallick and Mishra (2012) that study the doping of transition metals on NiO. They observed that the giant dielectric response when (Li, Fe) and (Li, V) doped NiO ceramic. This study proved that doping technique could increase the dielectric constant of NiO.

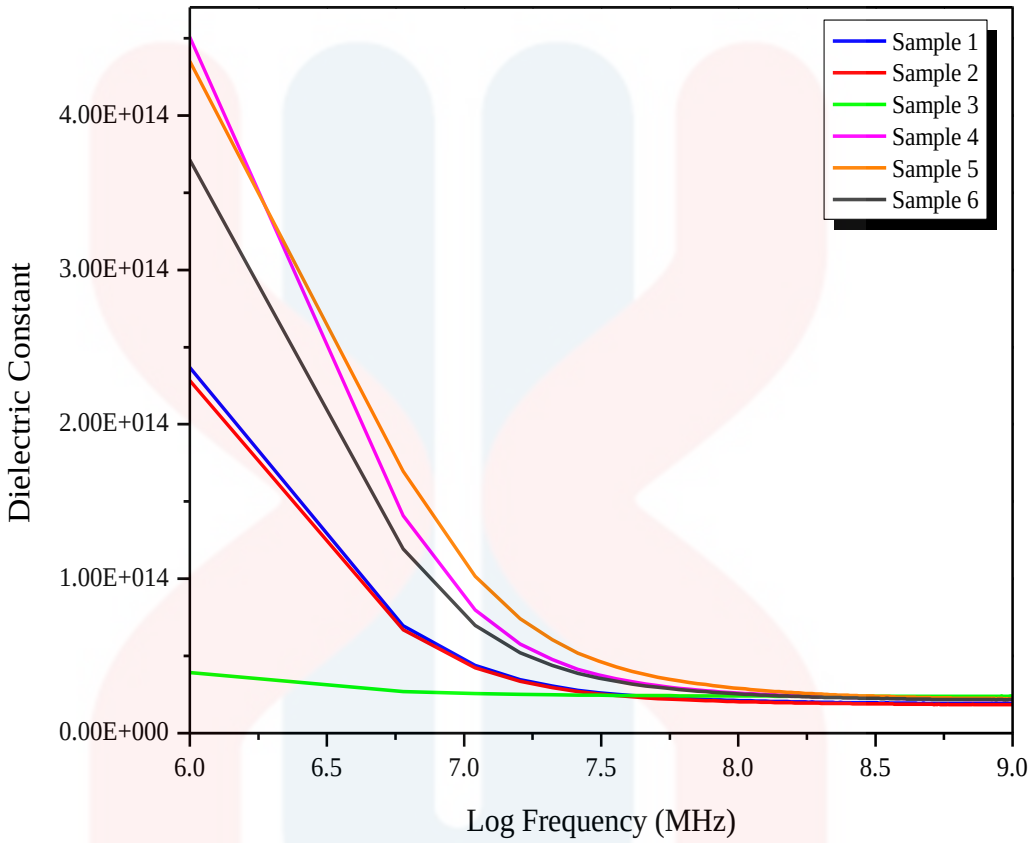

Figure 4.13: Frequency dependence of dielectric constant as a function of TiO_2 doping concentrations

Figure 4.14 shows the dielectric constant of $Ni_{1-x}Ti_xO_{1+x}$ samples with different TiO_2 doping concentrations at log frequency of 6 MHz. It is apparent that x = 0.03 mole %, which is Sample 4 exhibited highest ε_r, which was 4.51[14] at 6 MHz, while the lowest ε_r was Sample 3, which is x = 0.02 mole % with ε_r value of 3.93[13] at 6 MHz.

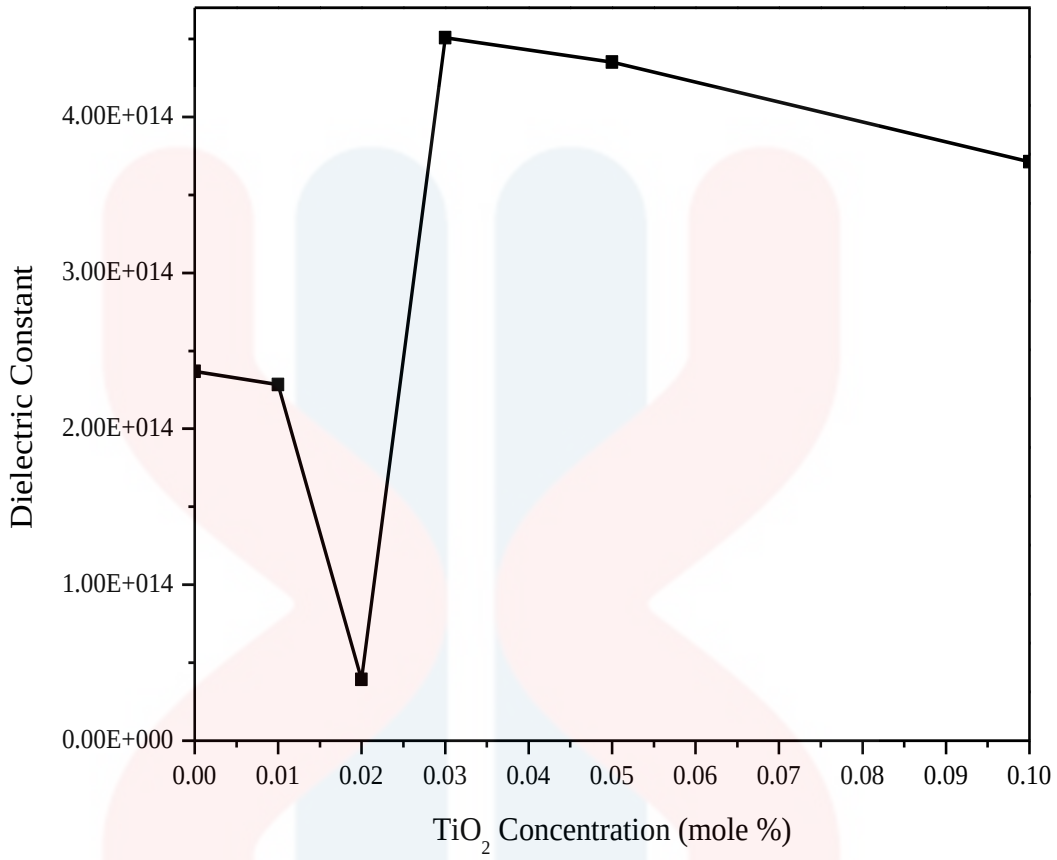

Figure 4.14: Dielectric constant as a function of TiO_2 doping concentrations at frequency of 6 MHz

Next, Figure 4.15 shows that dielectric loss (tan δ) for all concentrations of TiO_2 doped into NiO. However, when the frequency at 6 MHz, the lowest tan δ was at 0.05 mole % of TiO_2 with the value of 0.53, compared to undoped NiO with the value 0.71. The highest tan δ was 0.99 in Sample 3 with 0.02 mole % of TiO_2.

In addition, based on the previous study by Surendran et al. (2005), they claimed that the microwave dielectric properties of $MgAl_2O_4$ spinels were tailored by adding different mole fractions of TiO_2. The ε_r and Q factor of the mixed phases were increased with the molar addition of TiO_2 into the spinel to form mixtures based on (1-*x*)$MgAl_2O_4$-*x*TiO_2 (*x* = 0.0 - 1.0). This study proved that TiO_2 dopant is able to improve the dielectric properties.

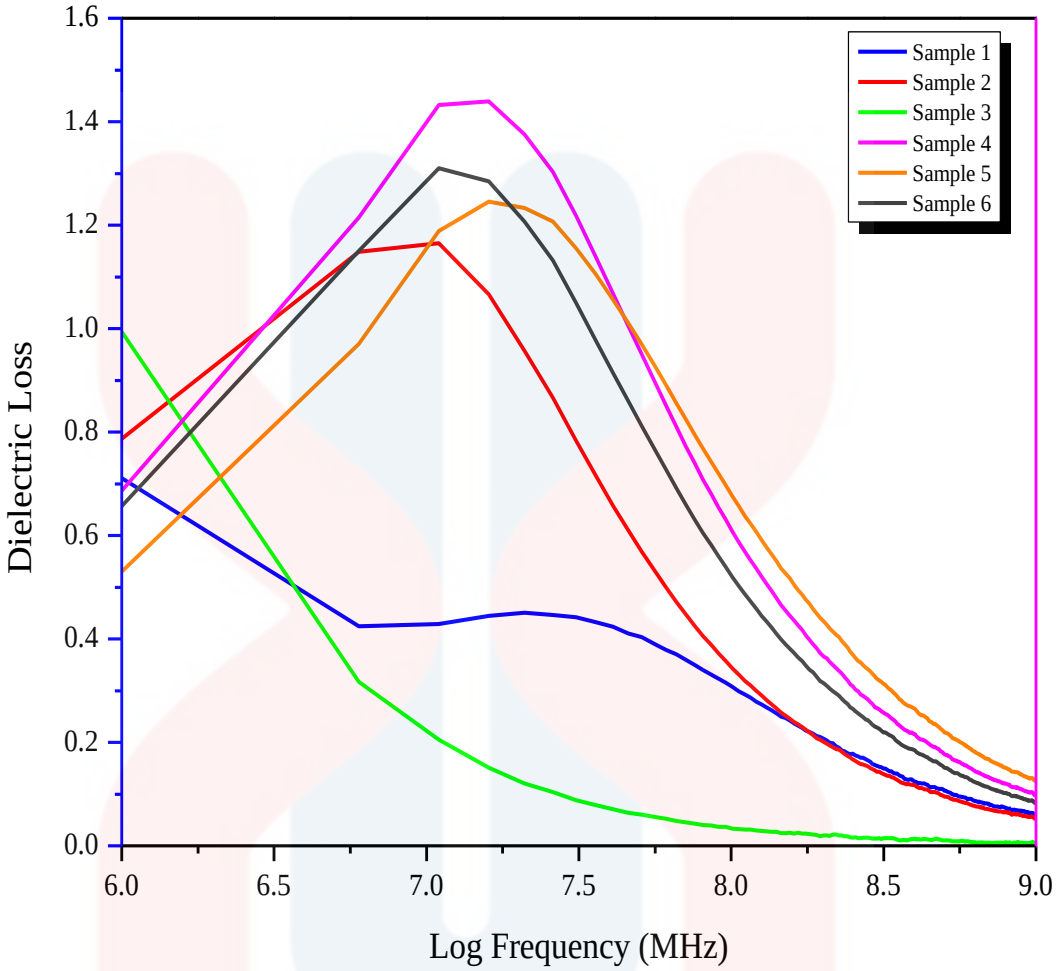

Figure 4.15: Frequency dependence of dielectric loss of $Ni_{1-x}Ti_xO_{1+x}$ samples as a function of TiO_2 doping concentrations

Figure 4.16 shows the dielectric loss of $Ni_{1-x}Ti_xO_{1+x}$ samples with different TiO_2 doping concentrations at log frequency of 6 MHz. It is apparent that, the lowest tan δ at 6 MHz was 0.53 in Sample 5, which is x = 0.05 mole % of TiO_2, while x = 0.02 mole % in Sample 3 exhibited highest tan δ, which was 0.99 at 6 MHz.

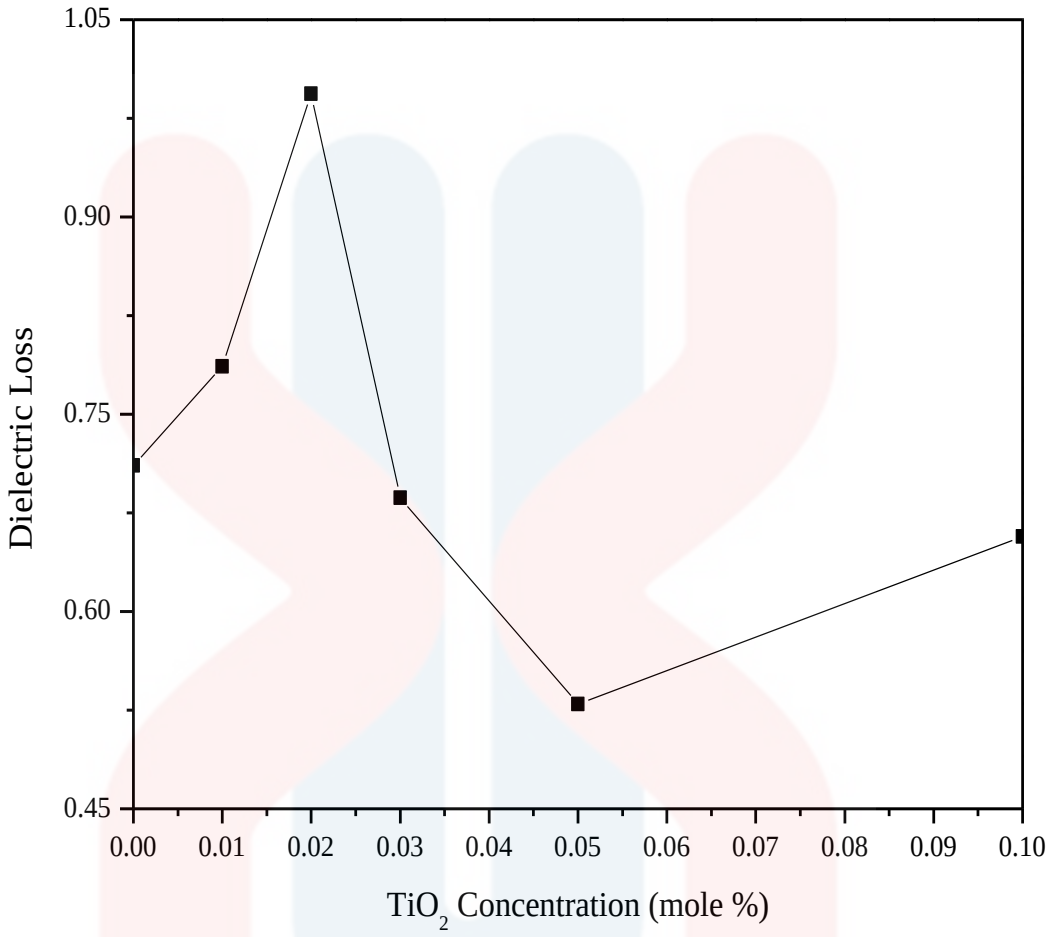

Figure 4.16: Dielectric loss of $Ni_{1-x}Ti_xO_{1+x}$ samples as a function of TiO_2 doping concentrations at frequency of 6 MHz

CHAPTER 5

CONCLUSION AND RECOMMENDATIONS

5.1 Conclusion

$Ni_{1-x}Ti_xO_{1+x}$ electroceramics was synthesized and characterized using solid-state method. XRD results of sintered samples produced a single NiO crystalline phase from Sample 1 to 3, which are represented pure NiO, 0.01 and 0.02 mole % of TiO_2 respectively, but there are small secondary phases of TiO_2 showed in Sample 4 to 6 as they represented the addition of 0.03, 0.05 and 0.10 mole % of TiO_2. SEM analysis showed that the grain sizes are getting larger with the addition of TiO_2 dopant. The largest grain sizes among those samples is in Sample 3, which is 0.02 mole % as the optimum TiO_2 content. Besides that, the amount of grain boundaries is increase as the TiO_2 content increase. Thus, this showed that the TiO_2 concentration increase, the bulk density decrease. For the dielectric test, the results come out with improvement of dielectric constant, ε_r by the addition of TiO_2 doping. The ε_r of undoped NiO is 2.37[14] at 6 MHz, while the ε_r of 0.03 mole % TiO_2 doped NiO at gives the result of 4.51[14] dielectric constant, which is the highest value among other doping content. In addition, the lowest dielectric loss, tan δ was at 0.05 mole % of TiO_2 with the value of 0.53, compared to undoped NiO with the value 0.71 and the highest tan δ was 0.99 when 0.02 mole % of TiO_2 was added. These results showed that different TiO_2 dopants gave the different effect in improving dielectric constant and dielectric loss. However,

throughout this study, overall can be conclude that the doping of TiO_2 is able to improve dielectric properties of NiO ceramic.

5.2 Recommendations for Future Research

In the future research of this study, there are some recommendations to improve this research project. Firstly, based on the shrinkage rate of the pellets, there should be an increasing shrinkage pattern toward the addition of TiO_2 content compared to the actual result in this study. However, in the next research, the researcher need to do further research on the shrinkage rate to get an increasing pattern. Other than that, the researcher can use different calcination and sintering temperature to find the optimum temperature that can improve $Ni_{1-x}Ti_xO_{1+x}$ properties. This is because heat treatment temperature and duration can give different effects on $Ni_{1-x}Ti_xO_{1+x}$ properties. Other than that, the research on synthesis of NiO can be done by using another method such as sol-gel method, chemical layer deposition and spray pyrolysis method. The researcher can compare the result by having these methods to get the best result of NiO properties. Besides that, the researcher can try to use different dopants to compare with TiO_2 dopant effects. The researcher may find another dopant that can give higher dielectric properties of NiO compared to TiO_2 as dopant.

REFERENCES

Albertst L. & Lee E. W. (1961). Magnetostriction in Antiferromagnetic Nickel Oxide. *Proc. Phys. Soc.*, 78, 728-733.

Aliahamad M., Rahdar A., Azizi Y. (2014). Synthesis of Cu Doped NiO Nanoparticles by Chemical Method. Journal of Nanostructures, 4, 145-152.

Aswal D. K., & Gupta, S. K. (2007). *Science and Technology of Chemiresistor Gas Sensors*: Nova Science Publishers.

Azelee W., Abu Bakar W., Yusuf Othman M., Ali R., Yong C., & Toemen S. (2009). The Investigation of Active Sites on Nickel Oxide Based Catalysts Towards the In-Situ Reactions of Methanation And Desulfurization. *Modern Applied Science*, 3(2), 35-43.

Azens A., Kullman L., Vaivars G., Nordborg H., & Granqvist C.G. (1998). Sputter-Deposited Nickel Oxide for Electrochromic Applications. *Solid State Ionics.*,113–115, 449–456.

Ba-Abbad M, Kadhum AH, Mohamad A, Takriff M. S. & Sopian K. (2012). Synthesis and Catalytic Activity of TiO2 Nanoparticles for Photochemical Oxidation of Concentrated Chlorophenols under Direct Solar Radiation. *Int. J. Electrochem. Sci.*, 7, 4871-4888.

Bandara J. & Weerasinghe H. (2005). Solid-State Dye-Sensitized Solar Cell with P-Type NiO As A Hole Collector. *Sol. Energy Mater. Sol. Cells*, 85(3), 385-390.

Barsoum M. W. (1997). *Fundamentals of Ceramics*, Chap 10, McGraw-Hill, New York.

Barsoum M. W. (2002). *Series in Materials Science and Engineering: Fundamental of Ceramics.* USA: CRC Press.

Broseghini M., Gelisio L., D'Incau M., Azanza R. C. L., Pugno N. M. & Scardi P. (2016). Modelling of the Planetary Ball-Milling Process. *The Case Study of Ceramic Powders. Journal of the European Ceramic Society*, 36, 2205-2212.

Ciesielczyk F., Bartczak P., Klapiszewski L., Paukszta D., Piasecki A. & Jesionowski T. (2014). Influence of Calcination Parameters on Physicochemical and Structural Properties of Co-Precipitated Magnesium Silicate. *Physicochem. Probl. Miner. Process. 50(1), 119−129*.

Fujii E., Tomozawa A., Torii H. & Takayama R. (1996) *Japanese Journal of Applied Physics*, 35, L328.

Hammami H., Arous M., Lagache M. & Kallel A. (2008). Electrical Conduction and Dielectric Properties in Piezoelectric Fibre Composites. *In Smart Materials for Energy, Communications and Security*, 169-189.

Hotový I., Huran J., Janík J., Kobzev A. P. (1998). Deposition and Properties of Nickel Oxide Films Produced by Dc Reactive Magnetron Sputtering. *Vacuum*, 5(12), 157–160.

Hsiao Y. J., Chang Y. S., Fang T. H., Chai Y. L., Chung C. Y. & Chang Y. H. (2007). High Dielectric Permittivity of Li and Ta co-doped NiO Ceramics. *Journal of Physics D: Applied Physics,* 40(3), 863.

Hussain M., Oku Y., Nakahira A. & Niihara K. (1996). Effects of Wet Ball-Milling on Particledispersion and Mechanical Properties of Particulate Epoxy Composites, Mater.Lett., 26 (3), 177–184.

Ibrahim S.S. & Selim A.Q. (2012). Heat Treatment of Natural Diatomite. *Physicochem. Probl. Miner. Process., 48,* 413–424.

Kamal H., Elmaghraby E. K., Ali S. A., & Abdel-Hady K. (2005). The Electrochromic Behavior of Nickel Oxide Films Sprayed at Different Preparative Conditions. *Thin Solid Films,* 483. 330-339.

Kingery W. D., Bowen H. K., & Uhlmann D. R. (1976). *Introduction to Ceramics,* 2nd edn, Wiley, New York.

Lei A., Guojia F., Longyan Y., Nishuang L., Mingjun W., Chun L., Qilin Z., Jun L., & Xingzhong Z. (2008). Influence of Substrate Temperature on Electrical And Optical Properties Of P-Type Semitransparent Conductive Nickel Oxide Thin Films Deposited By Radio Frequency Sputtering. *Applied Surface Science,* 254(8), 2401–2405.

Liu S., Wang J., Jia J., Hu X. & Liu S. (2012). Synthesis and Thermoelectric Performance of Li-doped NiO ceramics. Ceramics International, 38(6), 5023-5026.

Mallick P. & Mishra N. C. (2012). Evolution of Structure, Microstructure, Electrical and Magnetic Properties of Nickel Oxide (NiO) With Transition Metal Ion Doping. *American Journal of Materials Science,* 2(3), 66-71.

Marselin M. A. & Jaya N. V. (2015). Synthesis and Characterization of Pure and Cobalt doped NiO Nanoparticles. *International Journal of ChemTech Research,* 7, 6.

Motlagh M. M. K., Youzbashi A. A., & Sabaghzadeh L. (2011). Synthesis And Characterization Of Nickel Hydroxide Oxide Nanoparticles By The Complexation Precipitation Method. *International Journal of Physical Sciences*, 6, 6.

Moulson A. J., & Herbert J. M. (2003). Electroceramics: Materials,Properties, Applications. (2nd ed.).

Nan C. W., Wu J. B., Lin Y. H., Deng Y. (2002). *Phys. Rev. Lett.,* 89(21).

Patil K. C. (1993). Advanced Ceramics: Combustion Synthesis and Properties. *Bull. Mater. Sci.*16(6), 533-541.

Ponnusamy P. M., Agilan S., Muthukumarasamy N. & Dhayalan V. (2015). Effect of Chromium and Cobalt Addition on Structural, Optical and Magnetic Properties of NiO Nanoparticles. *Z. Phys. Chem.,* 0678.

Ren C., Qiu W., Chen Y. (2013) Physicochemical Properties and Photocatalytic Activity of The TiO_2/SiO_2 Prepared by Precipitation Method. *Sep. Purif. Technol.,* 107, 264–272.

Saruchi, Surbhi, Aghamkar, P., Kumar S. (2013) Neodymia-Silica Nanocomposites: Synthesis and Structural Properties. *Adv. Mater. Lett.*, 4, 78–81.

Sen S., Chakraborty N., Rana P., Sahu R., Singh S., Panda A. K., Tripathy S., Pradhan D. K., & Sen. S. (2016). Effect of Ti Doping on the Structural, Electrical and Magnetic Properties of $GaFeO_3$. Journal of Materials Science Materials in Electronics.

Shin W. & Murayama N. (2000). High Performance P-Type Thermoelectric Oxide Based on NiO. *Materials Letters*, 45(6), 302–306.

Stamataki M., Tsamakis D., Brilis N., Fasaki I., Giannoudakos A., & Kompitsas M. (2008). Hydrogen Gas Sensors Based on Pld Grown Nio Thin Film Structures. *Phys. Stat. Sol. (A)*, 205(8), 2064-2068.

Surendran K. P., Bijumon P. V., Mohanan P. & Sebastian M. T. (2005). $(1-x)MgAl_2O_{4-x}TiO_2$ Dielectrics For Microwave and Millimeter Wave Applications. *Appl. Phys. A*, 81, 823.

Tangwancharoen S., Thongbai P., Yamwong T. & Maensiri S. (2009). Dielectric and Electrical Properties of Giant Dielectric (Li, Al)-Doped Nio Ceramics. *Materials Chemistry and Physics*, Vol. 115(2–3), 585–589.

Thamaphat K., Limsuwan P. & Ngotawornchai B. (2008). Phase Characterization of TiO2 Powder by XRD and TEM. *Kasetsart. J. (Nat. Sci.)*, 42, 357-361.

Venter A., & Botha J. R. (2011). Optical and Electrical Properties of NiO for Possible Dielectric Applications, 107(1/2), 6.

Viruthagiri G., Praveen P., Mugundan S., & Gopinathan E. (2013). Synthesis and Characterization of Pure and Nickel Doped SrTiO3 Nanoparticles via Solid State Reaction Route. *Indian Journal of Advances in Chemical Science*, 3, 132-138.

Wang M., Tang Q., Yua C. & Cao M. (2011). Effect of ZrO_2 dopants on the sintering behavior and performance a mcmb-derived carbone laminations. Journal of Wuhan University of Technilogy-Mater. Sci. Edn. 1, 15-18.

Yijun S., Takashi E., Liangying Z., & Xi Y. (2002). High Anatase-Rutile Transformation Temperature of Anatase Titania Nanoparticles Prepared by Metalorganic Chemical Vapor Deposition. The Japan Society of Applied Physics, 41(2), 8B.

Zhang Y. R., Zhang B. P., Dong Y. & Li J. F. (2007). Effect of Ti Content on Microstructure and Dielectric Properties of Li and Ti Co-Doped NiO Thin Films. *Key Engineering Materials*, 336-338, 2639-2642.

ˇSepelák V., Bégin C. S., Le C. G. (2012). Transformations in Oxides Induced by High-Energy Ball-Milling, Dalton Trans, 41, 11927–11948.

APPENDICES

APPENDIX A

POWDER DIFFRACTION FILE OF NiO

Pattern: COD 9013980 Radiation: 1.54060 Quality: Quality Unknown

Formula	Ni0.995 O
Name	
Name (mineral)	Bunsenite
Name (common)	

Lattice:	Cubic	Mol. weight =	
S.G.:	F m -3 m (225)	Volume [CD] =	582.85
		Dx =	
		Dm =	
		I/Icor =	7.260

a =	8.35320	alpha =	
b =		beta =	
c =		gamma =	
a/b =	1.00000	Z =	
c/b =	1.00000		

d	2θ	I	h	k	l
2.41140	37.258	763	-2	-2	-2
2.08830	43.291	999	-4	0	0
1.47670	62.884	552	-4	-4	0
1.25930	75.423	266	-6	-2	-2
1.20570	79.417	164	-4	-4	-4
1.04410	95.083	76	-8	0	0

Figure A.1: Powder Diffraction File of NiO

APPENDIX B

POWDER DIFFRACTION FILE OF TiO_2

Pattern: COD 1010942 Radiation: 1.54060 Quality: Quality
Unknown

Formula	O2 Ti
Name	
Name (mineral)	Anatase
Name (common)	

Lattice:	Tetragonal	Mol. weight =	
S.G.:	I 41/a m d (141)	Volume [CD] =	130.36
		Dx =	
		Dm =	
		I/Icor =	5.670

a =	3.73000	alpha =	
b =		beta =	
c =	9.37000	gamma =	
a/b =	1.00000	Z =	4
c/b =	2.51206		

d	2θ	I	h	k	l
3.46550	25.686	999	-1	0	-1
2.39470	37.528	42	-1	0	-3
2.34250	38.396	150	0	0	-4
2.29830	39.165	76	-1	-1	-2
1.86500	48.791	247	-2	0	0
1.67450	54.777	158	-1	0	-5
1.64230	55.944	158	-2	-1	-1
1.47140	63.137	19	-2	-1	-3
1.45910	63.731	95	-2	0	-4
1.34380	69.951	66	-1	-1	-6
1.31880	71.478	54	-2	-2	0
1.25990	75.381	5	-1	0	-7
1.24600	76.372	83	-2	-1	-5
1.23250	77.363	23	-3	0	-1
1.17120	82.250	2	0	0	-8
1.15520	83.643	4	-3	0	-3
1.14920	84.179	34	-2	-2	-4
1.14380	84.669	16	-3	-1	-2
1.04400	95.095	6	-2	-1	-7
1.03600	96.066	20	-3	0	-5
1.02830	97.025	23	-3	-2	-1

Figure B.1: Powder Diffraction File of TiO_2

APPENDIX C

THE BULK DENSITY OF $Ni_{1-X}Ti_XO_{1+X}$

Calculation on bulk density of $Ni_{1-x}Ti_xO_{1+x}$ samples from Equation (3.4):

Bulk density, $\rho = \frac{\mathrm{D\ x\ } \rho(\mathrm{water})}{\mathrm{W - S}}$

Where,

$\rho_{(water)}$ = Density of Water (g/cm^3) = 1.00 g/cm^3

D = Dry weight, (g),

W = Saturated weight, (g),

S = Suspended weight, (g)

Table C.1: The bulk density of $Ni_{1-x}Ti_xO_{1+x}$

Sample	Dry Weight, D (g)		Suspended Weight, S (g)		Saturated Weight, W (g)		Bulk Density, ρ (g/cm^3)
	Readings	Average	Readings	Average	Readings	Average	
1	0.124	0.123	0.105	0.104	0.138	0.140	3.42
	0.121		0.103		0.140		
	0.123		0.103		0.141		
2	0.117	0.119	0.099	0.099	0.121	0.121	5.41
	0.118		0.097		0.120		
	0.121		0.100		0.121		
3	0.119	0.119	0.096	0.098	0.120	0.122	4.96
	0.117		0.099		0.122		
	0.120		0.098		0.123		
4	0.124	0.125	0.106	0.104	0.133	0.132	4.46
	0.126		0.101		0.132		
	0.124		0.105		0.133		
5	0.118	0.120	0.098	0.101	0.121	0.124	5.22
	0.120		0.102		0.125		
	0.121		0.099		0.125		
6	0.117	0.120	0.99	0.099	0.123	0.125	4.62
	0.123		0.99		0.125		
	0.121		0.98		0.126		

APPENDIX D

THE APPARENT POROSITY PERCENTAGES OF $Ni_{1-X}Ti_XO_{1+X}$

Calculation on apparent porosity of $Ni_{1-x}Ti_xO_{1+x}$ samples from Equation (3.5):

$$\text{Apparent porosity} = \frac{W-D}{W-S} \times 100\ \%$$

Where,

D = Dry weight, (g),

W = Saturated weight, (g),

S = Suspended weight, (g)

Table D.1: The apparent porosity percentages of $Ni_{1-x}Ti_xO_{1+x}$

Sample	Dry Weight, D (g)		Suspended Weight, S (g)		Saturated Weight, W (g)		Apparent Porosity Percentage (wt %)
	Readings	Average	Readings	Average	Readings	Average	
1	0.124	0.123	0.105	0.104	0.138	0.140	47.22
	0.121		0.103		0.140		
	0.123		0.103		0.141		
2	0.117	0.119	0.099	0.099	0.121	0.121	9.09
	0.118		0.097		0.120		
	0.121		0.100		0.121		
3	0.119	0.119	0.096	0.098	0.120	0.122	12.50
	0.117		0.099		0.122		
	0.120		0.098		0.123		
4	0.124	0.125	0.106	0.104	0.133	0.132	25.00
	0.126		0.101		0.132		
	0.124		0.105		0.133		
5	0.118	0.120	0.098	0.101	0.121	0.124	17.39
	0.120		0.102		0.125		
	0.121		0.099		0.125		
6	0.117	0.120	0.99	0.099	0.123	0.125	19.23
	0.123		0.99		0.125		
	0.121		0.98		0.126		

APPENDIX E

THE SHRINKAGE PERCENTAGES OF $Ni_{1-X}Ti_XO_{1+X}$

Calculation of shrinkage percentage of $Ni_{1-x}Ti_xO_{1+x}$ samples from Equation (3.6):

$$\text{Shrinkage percentage} = \frac{d1-d2}{d1} \times 100\ \%$$

Where,

d_1 = Diameter of pellet before sintering, (mm),

d_2 = Diameter of pellet after sintering, (mm)

Table E.1: The shrinkage percentages of $Ni_{1-x}Ti_xO_{1+x}$

Sample	Diameter Before Sintering, d_1 (mm)	Diameter After Sintering, d_2 (mm)	Difference of Diameter, d_1-d_2 (mm)	Shrinkage Percentage (%)
1	6.00	6.00	0.00	0.00
2	6.00	5.19	0.81	13.50
3	6.00	5.39	0.61	10.17
4	6.00	5.26	0.74	12.33
5	6.00	5.23	0.77	12.83
6	6.00	5.27	0.73	12.17